The University of Nottingham

UNITED KINGDOM · CHINA · MALAYSIA

Characterisations of Pre-Descemet's (Dua's) Layer for its Clinical Application in Keratoplasty

Saief Laith Muhamed Al-Taan

M.B.CH.B, MSC (Ophth)

Thesis submitted to The University of Nottingham for the degree

of Doctor of Philosophy in Ophthalmology

Supervisor

Professor Harminder S Dua

2018
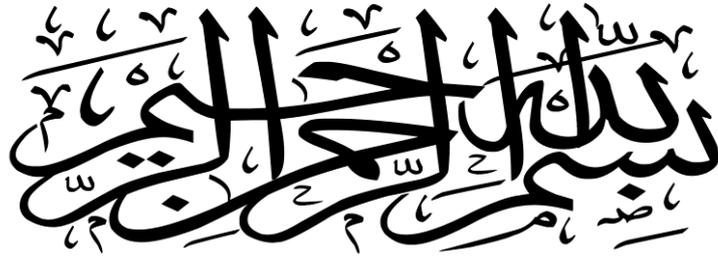
ABSTRACT

There exists a newly discovered, well defined, acellular, strong layer, termed pre-Descemets layer or Dua's layer (PDL), in the cornea just anterior to the Descemets membrane. This, with the Descemets membrane, separates along the last row of keratocytes in most cases of deep anterior lamellar keratoplasty with the big bubble technique. Recognition of this layer has considerable impact on lamellar corneal surgery, understanding of posterior corneal biomechanics and posterior corneal pathology, such as descemetocele, acute hydrops and pre-Descemets dystrophies.

The aim of this work was to understand the dynamics of big bubble formation in the context of the known architecture of the cornea stroma, ascertain how type 1 (air between deep stroma and PDL), type 2 (air between PDL and Descemets membrane) and mixed bubbles (combination of type 1 and type 2) form and measure the pressure and volume of air required to produce big bubbles in vitro, including the intra-bubble pressure and volume for the different types of big bubbles.

We also aimed to characterise the optical coherence tomography characteristics of the different layers in the wall of the big

bubbles to help surgeons identify bubbles and understand the structures seen by intra-operative OCT.

Finally we evaluated the endothelial cell density and viability in tissue samples obtained for Descemets membrane endothelial keratoplasty (DMEK) and pre-Descemets endothelial keratoplasty (PDEK) by the pneumodissection technique. Air was injected in 145 corneo-scleral samples, which were unsuitable for transplantation. Samples were obtained in organ culture medium from the UK eye banks and transferred to balanced salt solution ready for injection.

Different types of big bubble formed were ascertained. Air pressure and volume required to create the big bubble in simulated deep anterior lamellar keratoplasty were measured. It was found that PDL could withstand a high pressure before bursting at around 700 mm of Hg. Accurate measurements of type-2 big bubble proved challenging. The volume of the type-1 BB was fairly consistent at 0.1ml.

The movement of air injected in the corneal stroma was studied from the point of exit from the needle tip to complete aeration of the stroma and formation of a BB. This was video recorded and analysed. A very consistent pattern of air movement was observed. The initial movement was predominantly radial from the needle tip to the limbus, then circular in a clock-wise and

counter clock-wise direction circumferentially along the limbus, then centripetally to fill the stroma. All type 1 BB started in the centre as multiple small bubbles which coalesced to form a BB. Almost all type 2 BB started at the periphery near the limbus. Ultrastructural examination of the point of commencement of type 2 BB revealed the presence of clusters of fenestrations, which most likely allow air to escape from the otherwise impervious PDL to access the plane between PDL and DM. This was a novel discovery and explained how type 2 BB formed and why they almost always start at the periphery. The consistent pattern of passage of air was in concordance with the known microarchitecture of the central and peripheral corneal stroma.

Optical coherence tomography (OCT) characteristics of different types of big bubbles were studied. Samples obtained from the UK eye banks were scanned with Fourier-domain (FD-OCT), while that obtained from Canada eye bank were scanned with Time-domain (TD-OCT). A special clamp was used to affix the corneo-scleral sample on the OCT table with its posterior surface face the machine and mounted on artificial anterior chamber. It was found that FD-OCT could demonstrate type 1 BB wall as two parallel, double contour, hyper-reflective lines with hypo-reflective space in between. It also revealed that in type-2 BB, the posterior wall showed a parallel, double-contour curved hyper-reflective line with a dark space in between. This probably

corresponds to the banded and non-banded zones of DM. Dua's layer presents as a single hyper-reflective line. In TD-OCT, the posterior wall of type-1 and type-2 BB showed a single hyper-reflective curved line rather than the double-contour line. This finding will help cornea surgeons to identify and interpret different layers of big bubble intra-operatively with high resolution OCT devices.

Endothelial cell density of PDEK and DMEK tissue were calculated. Endothelial cells were counted using light microscope before pneumodissection. Air was then injected to ascertain the creation of type-1 and type-2 BB. Tissue was then harvested by trephination and endothelial cell density of both types were calculated again. It was found that the corneal endothelial cell count in PEDK tissue preparation is no worse, if not slightly better than, in DMEK tissue prepared by pneumodissection. Therefore, PDEK preparation represents a viable graft preparation technique.

LIST OF PUBLICATIONS RELATED TO THE WORK PRESENTED IN THIS THESIS:

1) AlTaan S.L., et al., Endothelial cell loss following tissue harvesting by pneumodissection for endothelial keratoplasty: an ex vivo study. Br J Ophthalmol, 2015. 99(5): p. 710-3.

2) AlTaan S.L, et al., Optical coherence tomography characteristics of different types of big bubbles seen in deep anterior lamellar keratoplasty by the big bubble technique. Eye (Lond), 2016 Nov:30(11):1509-1516.

3) Dua HS, Faraj LA, Kenawy MB, AlTaan S et al., Dynamics of big bubble formation in deep anterior lamellar keratoplasty by the big bubble technique: in vitro studies. Acta Ophthalmol, 2017 May 8. doi: 10.1111/aos.13460.

4) AlTaan S.L., et al., Air pressure changes in the creation and bursting of the type-1 big bubble in deep anterior lamellar keratoplasty: an ex-vivo study. Eye (Lond), 2017 Jun 30. doi: 10.1038/eye.2017.121.

5) Ross A, Said Dalia, Elamin A, AlTaan S.L., et al., "Deep anterior lamellar keratoplasty: Visco-bubbles and Air bubbles are different." Br J Ophthalmol. 2018 Apr 3. pii: bjophthalmol-2017-311349.

ACKNOWLEDGEMENT

I must also give thanks to my parents whom I have no words to acknowledge the sacrifices they made just to give me a shot at achieving my goal. Without their support and invocation, I would never have made it here. To my wife Zahraa, thank you ever so much for the love, encouragement and patience you have given me. To my awesome children; Omar and Fatima for the love and smile they have given me every day.

Finally, many thanks to all whose names do not appear and had a great contribution in the completion of this work.

CONTENTS

LIST OF FIGURES

LIST OF TABLES:

CHAPTER ONE

1. AN INTRODUCTION AND OVERVIEW OF KERATOPLASTY SURGERY

1.1 Corneal Anatomy

The cornea is a transparent, avascular and smooth tissue which is regarded as the main source of refractive power for the eye[1]. The significance of the cornea does not only relate to its refractive function, but it also works as a protective barrier from the outside environment and maintains normal intraocular pressure [1]. In order to achieve these functions, the cornea requires specific characteristics. For instance, for correct refraction a smooth and constant arch surface is essential. Transparency necessitates a thin avascular character. In contrast to this, the cornea requires strong and elastic components in order to contain the intraocular pressure and maintain its regenerative biological protection[1].

At birth, the cornea's size is large in comparison with the rest of the eye, its main growth then occurs between the sixth and eleventh month. The adult size of the cornea is reached between the first and second year [2].

The cornea has an elliptical shape with horizontal diameter measures (11.7 mm) and shorter vertical diameter (10.6 mm). The corneal thickness shows a discrepancy from the central zone (0.52 mm) to (0.67 mm) at the periphery [1]

The cornea consists of six layers which are: the epithelium (50-70 μm), Bowman's layer (8-14 μm), stroma (500 μm), Descemet's membrane (3-15 μm) and the endothelium (5 μm) [1]. Recently, Dua et al 2013 re-defined the human corneal anatomy by discovering new layer named as pre-Descemet's layer (Dua's layer).
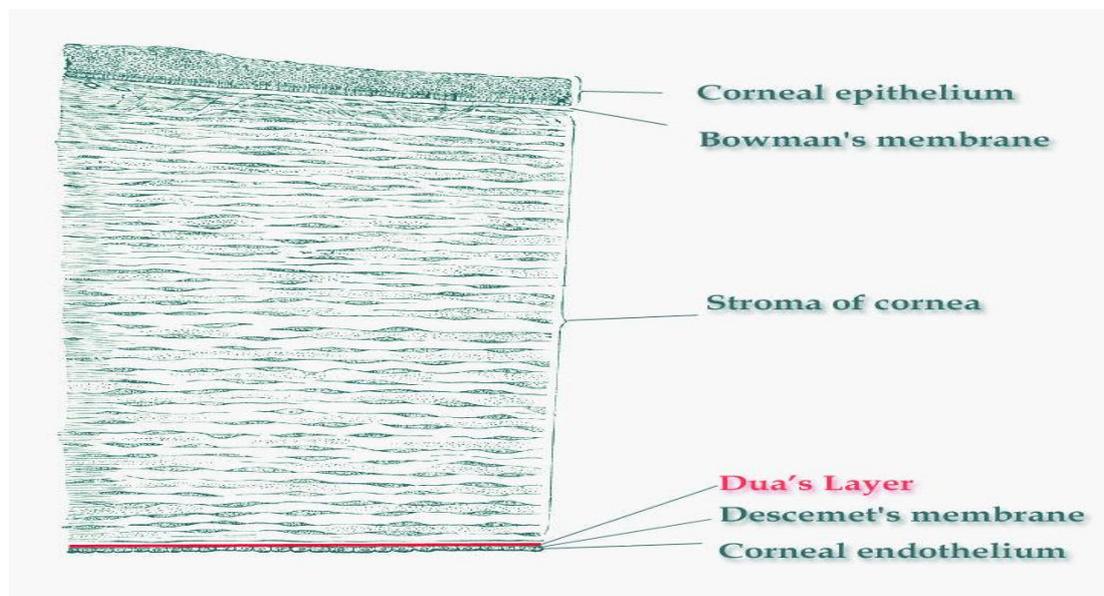
Figure 1.1 Cornea anatomy adapted from Gray's anatomy/ Sci- News 2013.

1.1.1 The epithelium

The corneal epithelium is stratified, non-keratinised and squamous. It forms around 10% of the whole corneal thickness.

The corneal epithelium is divided into three layers: superficial squamous layer, intermediate wing cell layer and deep basal cell layer. The surface epithelium is plate-like and is in a status of continuous flux throughout life with epithelial cells being replaced from the basal germ cells [1]. Epithelial turnover occurs every seven days by shedding the superficial epithelium into the tear film [2]. In the wing cells layer there is an increase in the intensity of interdigitations between cells and an increase in the number of desmosomes. The basal cells are tall, polygonal cells with an ovoid nucleus. Their basal membranes are smooth and appose to Bowman's layer being separated from it by their basal membrane. Hemi-desmosomes are areas of membrane specialization that act as an anchor of the basal cells to the basement membrane and Bowman's membrane [1]. The basal cells are characterised by their mitotic activity whereas the superficial cells are characterised by their high degree of differentiation [2].

1.1.2 Bowman's Layer

Bowman's layer is an acellular layer which is characterised by its anterior smooth surface that confronts the basement membrane of the epithelium and a posterior irregular surface which blends with the anterior stroma. The epithelial basement membrane reveals micro-irregularities with communications into bowman's layer[1]. The Bowman's layer consists of interwoven collagen

fibrils which are mostly of Type I collagen and a matrix of proteoglycans in which the collagen fibrils are embedded [1, 2].

1.1.3 Corneal stroma

The stroma represents about 90% of the corneal thickness. It consists of 200 to 250 stacked lamellae which extend from limbus to limbus and are superimposed on each other in such a manner that alternate layers cross at right angle [1].Some of these lamellae which are located anteriorly fuse with the Bowman's layer. However, majority of these bands run parallel to each other and to the corneal surface. Within each lamella the collagen fibrils run parallel to each other and each fibril runs the whole length of the lamellae. The predominant collagen of the stroma is Type I collagen[2]. Stromal collagen fibrils are uniformly arranged with a diameter of 320 to 360 Å, and a periodicity of 620 to 640 Å. In normal cornea, replacement of corneal collagen is a slow activity which may take about a year. While in case of wound healing the reconstruction process may take place in more rapid way but the diameter of the fibrils will be greater[1].

Stromal matrix is a translucent ground substance that consists of mucoprotein and glycoprotein. This ground substance fills all the space in the stroma that is not occupied by the fibrils or cells [1]. The stromal matrix compromises of fibroblastic cells called keratocytes, which produce extracellular matrix; and neural

tissue with its associated Schwann cells. In addition to Type I collagen which is present predominantly in the corneal stroma, there are other Types of corneal collagens such as III, V, and VI which are all seen in the cornea [2].

Corneal shape and relative stiffness is maintained by intertwining of collagen fibres running from anterior to posterior stroma and from centre to peripheral stroma to effectively keep the cornea as one fabric and control corneal shape. Other fibres make physical attachments both anteriorly to Bowman's layer and posteriorly to Descemet's membrane. These attachments keep corneal endothelium and epithelium cohesively and effectively attached[3].

1.1.4 Pre-Descemet's layer (Dua's Layer):

In 2013 Dua *et al.* stated that "there exists a novel, well–defined, acellular, strong layer in the pre-Descemet cornea". This layer contains mainly collagen I in addition to collagen IV and VI which are more in this layer than that of the corneal stroma which explains the difference between this layer and the stroma. CD34 is a keratocyte cellular marker which is found to be negative in this layer indicating the absence of keratocytes [4]. Recently, Electron microscopy has shown that beams of collagen emerge from the peripheral border of Dua's layer on the anterior surface of Descemet's membrane and continue to divide

and subdivide to become the beams of the trabecular meshwork [5]. Trabecular cells were recognised in the peripheral circumference of Dua's layer and corresponded to the split-up of the collagen fibrils of Dua's layer [5]. Recognition and studying the physical characteristics of this layer will have significant impact on posterior lamellar graft transplantation and understanding of posterior corneal pathology such as Descemetocele, acute hydrops and pre-Descemet's dystrophies and the knowledge of the dissection plane of this layer will allow it to be exploited for endothelial keratoplasty. Furthermore, recognition of this newly discovered layer will help understanding of corneal dynamics through testing the spread of air within the stroma during air injection [4].

1.1.5 Descemet's membrane

Descemet's membrane is laid down/deposited by the endothelial cells during the fourth month of gestation, forming a thick basal lamina which consists of anterior banded and posterior non-banded portions. Descemet's membrane is considered as the basement membrane of the corneal endothelium. The 3 μm banded layer exists in the foetus and seems to be constant in thickness after birth, whereas the basal non-banded layer increases in thickness from 2 μm up to 10μm throughout an individual's lifetime[2].Descemet's membrane can be separated easily from the endothelium and the posterior stroma. The latter

cleavage is being applied in lamellar keratoplasty for Descemet's membrane endothelial keratoplasty (DMEK). When incised or torn, the Descemet's membrane curls like a scroll with the endothelial cells on the outside of the scroll. This illustrates the elastic properties of the membrane [1].Descemet's membrane progressively increases in thickness throughout life and a differential staining response of the membrane is also noticed with the anterior third (banded layer of the membrane)staining darker. Descemet's membrane consists of atypical fine collagen fibres, which are of 100 Å in diameter and amorphous ground substance [1]. Immunohistochemical studies show that this basal lamina contains fibronectin, Type IV collagen, and laminin which are present in both layers of Descemet's membrane [2]. The organisation of Descemet's membrane gives it a greater tensile strength than other parts of the cornea. This is obvious in some of the pathological conditions which lead to erosive changes in the stroma and leave the membrane only to tolerate the intraocular pressure. If Descemet's membrane is torn it can be regenerated by the endothelial cells[1].

1.1.6 Endothelium

The endothelium consists of single layer of hexagonal cells that are 4 to 6 microns thick and 20 microns in width. In humans the endothelial cells do not regenerate although in lower mammals

they reveal mitotic activity[2]. Furthermore, in advancing age these cells become less ordered (pleomorphism and polymegathism) [2]. It seems that there are no obvious adhesive connections between the endothelium and the Descemet's membrane and that the intraocular pressure has supportive effect to the endothelium [2]. The endothelial cells play an important role in maintaining the transparency of the cornea. This is because the endothelial cells can control the corneal hydration as their cytoplasm contains numerous pinocytotic vesicles [1].

1.2 Embryology

corneal development is started by separation of the lens vesicle from the ectoderm by day 33 of the gestation [6]. The epithelium develops first as a single layer of ectoderm covering the optic cup and the lens vesicle [1]. By the fourth month of gestation the epithelium consists of three Types of cells: small cells with several microvilli; medium-sized cells with less surface microvilli; and large cells with fewest surface projections. Adult appearance of human corneal epithelium is reached by the fifth to sixth month of gestation [6]. During the seventh week of gestation, further migration of the mesenchymal cells occurs and extends between the epithelium and endothelium and go on to

form the stroma, which continues to develop over the next two months [1].

Initially the central stroma is an acellular zone, the developing cells then differentiate to form fibroblasts or keratocytes, which are responsible for the secretion of Type I collagen and the stromal matrix. By the eighth week of gestation the central stroma consists of five to eight stromal layers and the most posterior layers confluent at the periphery with the mesenchymal tissue of the sclera [6].

During the fourth month of gestation a thin acellular layer appears between the basement membrane of the corneal epithelium and the lamina propria, this lamina later forms Bowman's layer [7] During the third month, the endothelium develops as a single layer of low cuboidal cells which rest on the basal lamina and forms the Descemet's membrane [6]. During the same period, the Descemet's membrane is formed from collagenous material adjacent to the mesothelium [7]. Further differentiation of Descemet's membrane forms a multi-layered structure which consists of ten layers by the sixth month and thirty to forty layers at birth. The anterior part of Descemet's membrane is characterised by its unique organisation and has a maximum thickness of 3µm at birth, known as foetal banded zone. The posterior portion the membrane which consists of

fibrillogranular material and continues to grow throughout life is called the non-banded zone [6]. At birth, the Descemet's membrane is thin and increases in thickness after delivery due to growth of its posterior zone [7].

The first wave of the migration of the neural crest cells passed between the primary stroma and the lens vesicle to form the endothelium. The second wave of the neural crest cells forms the iris and pupillary membrane. The third wave migrates to the primary stroma and forms the precursor of the keratocytes which will form the definitive secondary stroma [8].

The primary stroma is compressed anteriorly and believes to form the basis of Bowman's layer. However, posteriorly it is responsible for the characteristics of the posterior part of the stroma, the DL. Just like the Bowman's membrane which preserves its collagen from the epithelium. The DL is also influenced by the endothelium due to its proximity to the DL [8].

1.3 Corneal innervation

The cornea is one of the most highly innervated tissues in the human body. The corneal epithelium is the most densely innervated among all epithelia. It receives around 300-400 more nerve fibres a unit area than that of the epidermis. The corneal

nerve supply is mainly sensory and is derived from the trigeminal nerve and is carried by its ophthalmic division [9]. Forty four thick nerves enter the cornea in relatively equal distribution approximately 1 mm outside the limbus. Most of them are in continuation with the suprachoroidal nerves. Corneal nerve bundles enter the stroma in predominantly its middle and deep parts. Nerve bundles lose their myelin sheath before or soon after entering the stroma. This help to maintain corneal transparency. Limbal nerve fibres enter the corneal quadrants in different numbers as follows: superiorly (11.0), medially (9.43), inferiorly (11.43), and laterally (11.86), with an average overall innervation of 43.72. From the stoma, nerve fibres turn toward Bowman's layer. Sub-Bowman's nerves which are located in the most anterior part of the stroma penetrate through Bowman's layer predominantly at the mid-peripheral cornea to form sub-basal (epithelium) nerves. Before their penetration of Bowman's layer, sub-Bowman's nerves divide into two or more branches which terminate in bulb like structures in the sub-basal plane giving a 'branching and budding pattern' (Figure 2). From each 'bulb' sub-basal nerves arise varying in number from a single filament to a leash of several neurities. These extend and run as linear structures running in the sub-basalcornea. .[10]. Nerve leashes run obliquely in between the epithelial cells ending in the outer squamous cells [9].
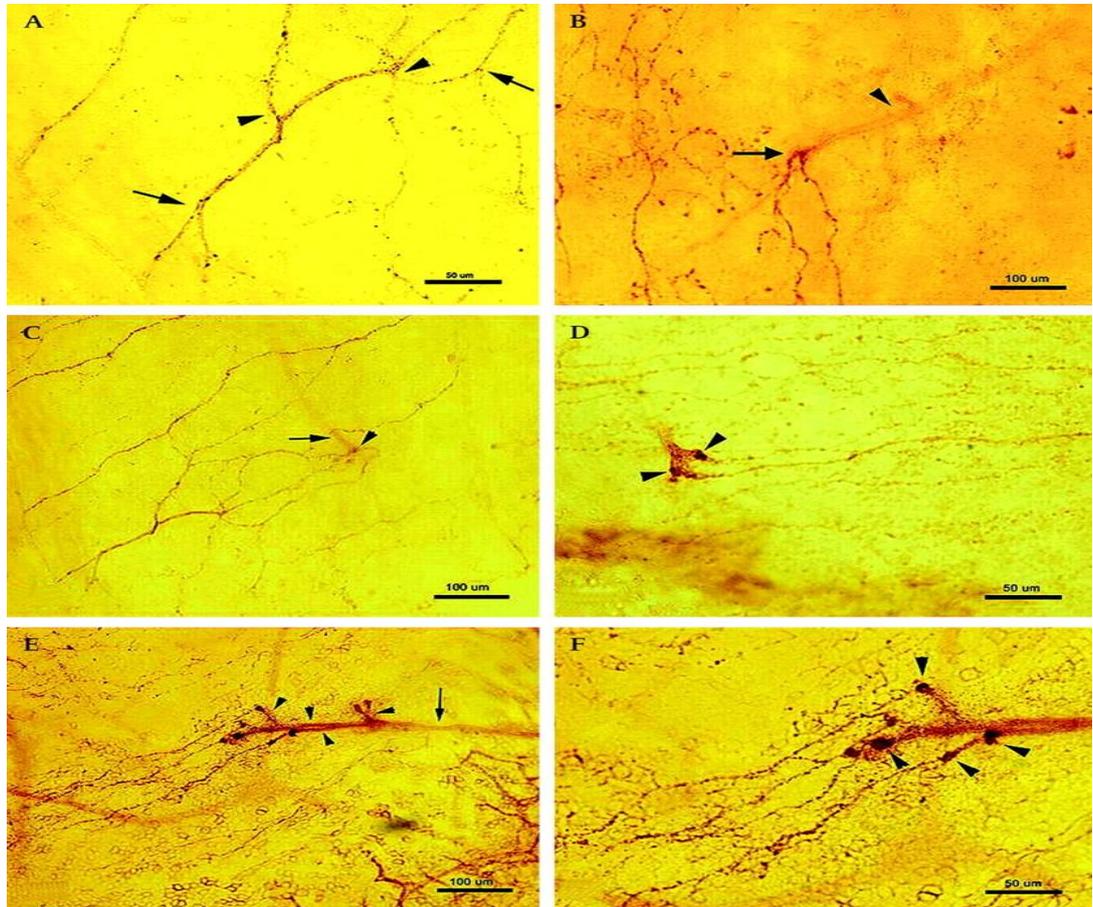
Figure 1.2 Corneal innervation. Photomicrographs of whole human corneal mount stained by the acetylcholinesterase technique. (A) sub-basal nerve plexus with characteristic branching (arrows) and union/re-union (arrowheads). The nerves contain densely stained fine granular material. (B) sub-basal epithelial leashes of nerves in a human cornea. The arrow shows the point at which a sub-Bowman's nerve penetrates Bowman's zone giving rise to multiple sub-basal nerves. The sub-Bowman's nerve is out of focus in this microscopic image (arrowhead). (C) A thicker sub-Bowman's nerve (arrow), which reaches the epithelium at the site of perforation (arrowhead) giving rise to multiple thinner sub-basal nerves. (D) A sub-Bowman's nerve bifurcates and penetrates to emerge anterior to Bowman's zone terminating in discoid or bulbous thickenings (arrowheads) which give rise to sub-basal nerves. (E) A single sub-Bowman's nerve (arrow) gives multiple branches (arrowheads) just before perforating the Bowman's zone 'budding and branching pattern'. (F) A higher magnification of the same nerve in figure (E) showing characteristic bulb like thickenings at the perforation site (arrows) from which sub-basal nerves arise. Scale bars,50 mm (A, D, F) and 100 mm (B, C, E). Adapted from Al-Aqaba et al 2014.

1.4 Cornea as a lens

The cornea represents the major refractive tissue of the eye. It represents two-third of the refraction of the eye with a total of +43 dioptres. This is mainly due to its anterior surface which has a refractive power of 48 dioptres, while the posterior curvature has a refraction of -5 dioptres. So the total optical contribution will be 43 dioptres [11].

Spherical aberration is defined as when a beam of rays passing through spherical lens the peripheral rays will deviate more than those passing through the paraxial zone of the lens. Corneal aberration can cause image distortion due to increase in prismatic effect of the cornea at the periphery, also oblique astigmatism and come aberration may occur due to focusing of the rays passing through the periphery near the principle axis. [12]. Most experimental studies of the cornea suggest that the anterior corneal surface has the main contribution of the corneal aberration, but the total aberrations of the eye is lower than that of the cornea alone, because of the internal optics which tend to compensate the internal aberrations. This property tends to change with age due to slight peripheral thinning [11]. Also, human cornea can reduce this effect by the fact that anterior corneal surface is flatter at the periphery than at the centre so that acts as aplanatic surface [12].

1.5 Dua's layer: discovery, characteristics, clinical applications and controversy

1.5.1 Discovery

In 2007 and at the annual congresses of the Royal College of Ophthalmologists and the Societa Italiana Cellule Stiminalie Superficie Oculare, Professor Harminder S Dua presented his preliminary data which hypothesized the existence of a 'pre-Descemet's (stromal) layer' [8].

In 2013, Dua et al published their data and concluded that there exists a novel, well-defined, strong, acellular layer at the pre-Descemet's cornea [4]. Dua et al proposed that the cleavage plane in BB DALK was not between the Descemet's membrane and the stroma but between the deep stroma and a pre-Descemet's layer (Dua's layer) [8].

1.5.2 Characteristics of Dua's layer

Dua's layer characterised by 5-20 µm thickness as revealed by the light and electron microscopic and immunologic studies of the layer. It is made of 5-11 compact lamellae of collagen fibres, type 1 collagen constitute the predominant collagen of the layer in addition to type 4 and 6 which are relatively more in the layer than in the stroma. Also, it has high content of the elastin like

network which is abundant in the 10 μm above the DM [13]. The cleavage occurs along the last row of the stromal keratocytes but the layer is acellular (paucity of keratocytes). Electron microscope shows increased expression of type 6 long-spacing collagen. After peeling off the DM in type-1 BB, the bubble did not deflate and air was within the DL and the posterior stroma which means that the layer is impervious to air, and when ablated by excimer laser, a type 1 big bubble cannot be created. The layer is continuous with the trabecular meshwork and possesses high tensile strength [8].

1.5.3 Clinical application of Dua's layer

The knowledge about the characteristics of Dua's layer has helped surgeons in many clinical applications as follow:

- Dua's layer helps providing a cleavage plane - accessed by air or mechanically - and it is easily handled in lamellar keratoplasty [8].

- It forms the posterior wall of type-1 BB, which is of rough appearance. This helped to explain the difference between type1 and type-2 BB which has smooth and featureless appearance. Also, it helped to understand the mixed bubble which is formed

from cleavage between DL and DM but not between banded and non-banded zone of DM [8].

- It explains the mechanism air enters the anterior chamber during Big Bubble DALK. The understanding of the microanatomy of the posterior cornea in terms of the different types of BBs has improved the understanding of the deep anterior lamellar keratoplasty and made it safer [8].

- It improves understanding of the posterior corneal pathologies such as Descemetoceles and macular corneal dystrophy. In the former it can be covered with a Dl which provides strength and delays rupture. In the later the DL is affected and thus opacities may remain after DALK. On the same time endothelial involvement is also evident in macular dystrophy, thus DL could be swayed by the endothelium [8].

 - It forms the basis of innovations in cornea surgery:

Pre-Descemet's endothelial keratoplasty (PDEK): wherein DM and DL are used as donor graft for endothelial transplantation [8].

 Triple Deep anterior lamellar keratoplasty (DALK): DALK plus phacoemulsification plus implant [14].

Surgical management of acute hydrops: Dua et al hypothesized that a tear in DM and DL is the cause of acute hydrops in

keratoconus. Professor Muraine's group proved this hypothesis and revealed that rapid reduction in corneal oedema can be achieved by suturing the tear in DL in patients with acute hydrops [15].

1.5.4 Controversy

Dua's layer has become widely accepted as an important part of the corneal anatomy. However, there was ongoing debate about the name of the layer (Dua's layer); on whether it is a discrete layer or part of the stroma; and the relation of the keratocytes to the layer.

The naming of the layer on behalf of professor Dua was not intentional. The controversial issues which are existed from some quarters were mainly spurred by the media coverage. However, during the course of work on the layer, co-workers referred to it as 'Prof's Dua's layer'. When the original manuscript was written the name Dua's layer was not part of it. Latter on the name has passed through the editorial process of the journal of Ophthalmology without any comment on the name. Notwithstanding this, the name Dua's layer has become the keyword in many textbooks such as Oxford of Ophthalmology and Kanski's Clinical Ophthalmology. In addition to thousands of references which make it impossible to turn the back the clock [8].

Dua's layer separates consistently from the rest of the stroma. This suggests that it is not a random separation of the stromal collagen during Big Bubble DALK.

Regarding the ongoing debate about the presence or absence of keratocytes in DL, Recently Kruse et al [16] and Jester et al [3] have reported the presence of keratocytes within 5 µm of the DM. However, they did not mention the density of the keratocytes in relation to the layer. Also they did not comment on the number of keratocytes seen on the stroma of DL compared to that on it. Dua et al stated that there is no evidence in the literature showing the location of keratocytes on the DM [8]. Additionally, there is a cell-free zone immediately anterior to the DM [17]. Dua et al has reported that the cleavage occurs along the last row of keratocytes [4]. 'Hence a row is not a line through each keratocyte but rather a line connecting all the posterior keratocytes, that is, the last row of keratocytes' [8].

1.6 History of Corneal transplantation

The nineteenth century witnessed several attempts to replace the opaque human cornea by healthy one. Sadly most of the efforts faced a failure not because of the lack of ideas on how to perform the keratoplasty procedure but due to the deficiency of

the knowledge of the physiology immunology and pathology of the cornea which would prevent the graft rejection. However, these trials gave way to despair until the first successful corneal graft was done by Dr Eduard Zirm in 1905 where the transplanted cornea remained clear. He reported his case in 1906, and despite his success in performing several keratoplasties, he never published any of his work. During the next 30 years, keratoplasties were done using tissue from enucleated eyes of living donors. However, the main causes of failure were graft detachment and subsequent opacity. [18].

In the 1940s, dramatic evolution of corneal transplantation was obvious due to the development of eye banking. Richard Townley Paton established the eye bank of sight restoration which was the world's first eye bank in New York. Not only this, the development of new instruments such as the trephine, and the concepts of tissue handling and preparation helped to improve corneal transplantation. Moreover, the invention of antibiotics, corticosteroids, viscoelastic and suture materials all these equipment helped in the success of this type of surgery [18].

In 1955 Vladimir Filatov, a Russian ophthalmologist started a systemic study on corneal grafts, where he had done 3500 successful human keratoplasties. Also, he worked on the development of many technical instruments and devices which

helped to overcome the intricacies and complications of this operation. Filatov supported the use of cadaver corneas and the egg membrane as a graft and is thus considered as the "grandfather of eye banking". He also reported the crucial points in corneal suturing and protection of the intraocular tissue during trephination of the cornea[18].

1.7 Indications of Corneal Transplantation

Corneal grafts are used to treat a variety of corneal diseases such as corneal ectasias, stromal abnormalities, endothelial dystrophies and corneal infection. The incidence of corneal diseases varies during the last years, for example; Fuchs endothelial dystrophy has increased in the elderly population, while the prevalence of pseudophakic bullous keratopathy may have changed after the existence of phacoemulsification [19].

The main indications for corneal transplantation can be categorized into the following Types: corneal ectasias (keratoconus and acute hydrops), stromal abnormalities (stromal dystrophy and stromal opacity), endothelial failure (Fuch's endothelial dystrophy, pseudophakic bullous keratopathy, and aphakic bullous keratopathy), infection (bacterial, viral, protozoan, fungal and others), graft rejection and re-graft, in addition to other lamellar indications [19]. In the

UK from 1999 to 2009, keratoconus represented approximately 25% of total graft operations [19].

However, the percentage of corneal grafts for the treatment of endothelial failure during the same period has increased and represent around one-third of the total keratoplasty operations in the UK. The percentage of corneal grafts for the purpose of endothelial failure is increasing due to the increase of Fuch's endothelial dystrophy among the old people in the UK, whereas people which are require keratoplasty for the bullous keratoplasty still unchanged, which may be due to the improvement of cataract surgery and the wide spread use of phacoemulsification and subsequent corneal protection [19]. Corneal infections remain the lowest cause of corneal transplantation occupying 8% of all the corneal grafts performed [19].The proportion of keratoplasty surgery due to graft rejection increased to around15 % within the same period [19].

To summarise, that the main indications for corneal transplantation was endothelial failure, second indication was keratoconus which is followed by re-grafts surgery due to rejection. Corneal infections had the least percentage of corneal graft workload.

1.8 Penetrating keratoplasty (PK)

Penetrating keratoplasty has been regarded as the gold standard for the management of advanced keratoconus because of its safe and effective technique which provides good optical and visual outcomes. The procedure is based on the replacement of the entire thickness of the diseased cornea with healthy transparent one [20, 21].
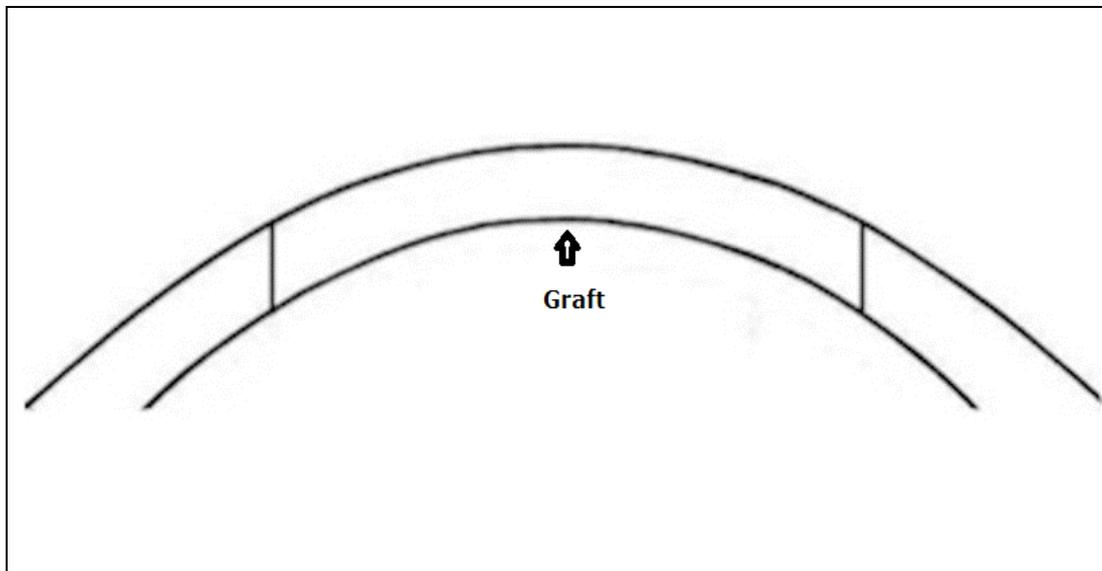
Figure 1.3 Penetrating keratoplasty adapted from Massimo Busin et al 2015.

Penetrating keratoplasty can be performed for any indications including stromal and endothelial diseases with resultant good optical outcomes as there is no lamellar interface problems and relatively undemanding procedure [22].

However, 'this procedure should be reserved for patients who do not tolerate contact lenses or do not get needed visual acuity with contact lenses because of complications [23].

1.9 Risks of Penetrating keratoplasty

Several studies are published discussing the main postoperative complications of penetrating keratoplasty. Olson et al reported that in ninety three cases, allograft reaction happened in 36 cases and seven of them had similar recurrent reactions [23]. In the same sample study, the best corrected visual acuity was 20/25 or better in seventy two cases and the mean astigmatism was 2.7 dioptre. Intraocular pressure was another postoperative complication, sixteen patients exhibited an elevated intraocular pressure after surgery, and the highest IOP was 42mmHg. Another 15 cases revealed elevated IOP with as high as 33mmHg. Punctate keratitis was another postoperative drawback of penetrating keratoplasty in seven patients of the same group.

Penetrating keratoplasty may cause several complications which are unique to this type of corneal graft surgery. These complications include: donor graft rejection which remains the most common cause of graft failure, prolonged steroid use which may predispose to cataract and glaucoma, microbial endophthalmitis, iris and lens damage due to trephination, open

eye complications such as choroidal haemorrhage and positive vitreous pressure, wound complications such as flat anterior chamber from wound leakage, anterior chamber epithelial ingrowth, and accelerated donor graft endothelial cell loss. Additionally, graft-host junction may disrupt easily by trivial trauma even long time after surgery [8, 20].

Suture removal after PK can take longer than other Types of keratoplasty. In addition to other suture-related problems such as: abscess formation at the site of sutures, delayed epithelialisation, induced post-operative astigmatism, early stich loosening, delayed absorption and unpredictable breakage. Corneal dystrophies may recur after penetrating keratoplasty, and usually involve the anterior part of the graft [20].

1.10 Evolution of deep anterior lamellar keratoplasty (DALK)

In the seventh decade of the 20th century, there was increased interest in lamellar keratoplasty. Some ophthalmic surgeons such as Anwar, Malbran and Paufique used lamellar surgical transplants as an alternative to penetrating keratoplasty for optical correction of axial corneal diseases with intact endothelium, such as keratoconus, corneal ectasia, corneal scar, stromal corneal dystrophies or infection. One of the most publicised lamellar keratoplasty procedures was DALK, which involves removal of the central corneal stroma, leaving the endothelium and Descemet's membrane intact. Preserving the recipient's corneal endothelium, this will prevent any potential endothelial immune rejection and maintain most of the recipient endothelial cell density [20].

Sugita and Kondo who were the first described their technique for Descemet's membrane baring. They called this procedure "deep anterior lamellar keratoplasty" [20].

DALK procedure refers to removal of the whole or nearly whole of the corneal stroma while keeping underneath healthy endothelium and Descemet's membrane [20]. Consecutively, this will reduce the host endothelial loss after surgery, in addition to better visual rehabilitation if compared with PK. The intraoperative complications associated with open sky segment,

and extra-operative complications are usually less in DALK including: haemorrhage, anterior synechia, endophthalmitis and iris prolapse [24].

The main advantages of DALK over PK are the following: Immune rejection from endothelium not occurs, it is extraocular procedure, topical steroids can be used for period shorter than with DALK, there is less loss of endothelial cell density, in comparison with PK; it possesses more resistance to rupture of the globe after blunt trauma and Removal of sutures can be earlier in DALK than PK [20]. However, PK is the preferable procedure with resultant good optical outcomes as there is no lamellar interface problems and relatively undemanding procedure[22].

Surgical techniques:

(A) Direct Open Dissection: Anwar was the first ophthalmic surgeon who described this method in 1972. He performed a partial thickness trephination of the cornea which is followed by lamellar dissection using 69 beaver blade and Martinez spatula or varieties of other types of dissecting blades. This dissecting method of the deep stromal layers places the Descemet's membrane at a risk of rupture [24, 25].

(B)   Dissection with Hydrodelamination: This method first described by Sugita and Kondo. In this technique intrastromal fluid injection is performed after trephination and lamellar dissection. Then saline is injected into the stromal bed by 27-gauge needle. This will swell the stroma causing deep dissection safer and minimise the risk of DM rupture. However, perforation still occurs in this method (39.2% in one of the studies) [24, 26].

(C)   Melles Technique (Closed Dissection): this technique described by Melles et al in 1999. It facilitates deep lamellar dissection by using special spatula, thus creating deep, long stromal pocket. This can be enlarged by using side movement of the spatula, or injection of viscoelastic. Suction trephine is used to enter the viscopocket, and the above stroma then excised. The donor stroma is then sutured in place after removal of DM. Ruptured DM is reported in 14% of the reported cases [24, 27].

(D)   Anwar's Big Bubble Technique: In 2002 Anwar and Teichmann described the big bubble technique. Since then it has gained its popularity. Where about 60-80

% of the cornea is trephined and dissected, and then air is injected by using 27 or 30 gauge needle or special cannula to produce a "big bubble" and separate the DM from the stroma. The stroma then removed and the DM is bared. The donor tissue is placed and sutured after removal of donor DM [24, 28, 29].

(E) Big Bubble Technique Combined with Femtosecond laser: In this technique a femtosecond laser is used to dissect the anterior lamella. This allows mushroom or zigzag configuration of the corneal wound in both patient and the donor, to improve wound strength, reduce postoperative astigmatism and allow early suture removal [24, 30].
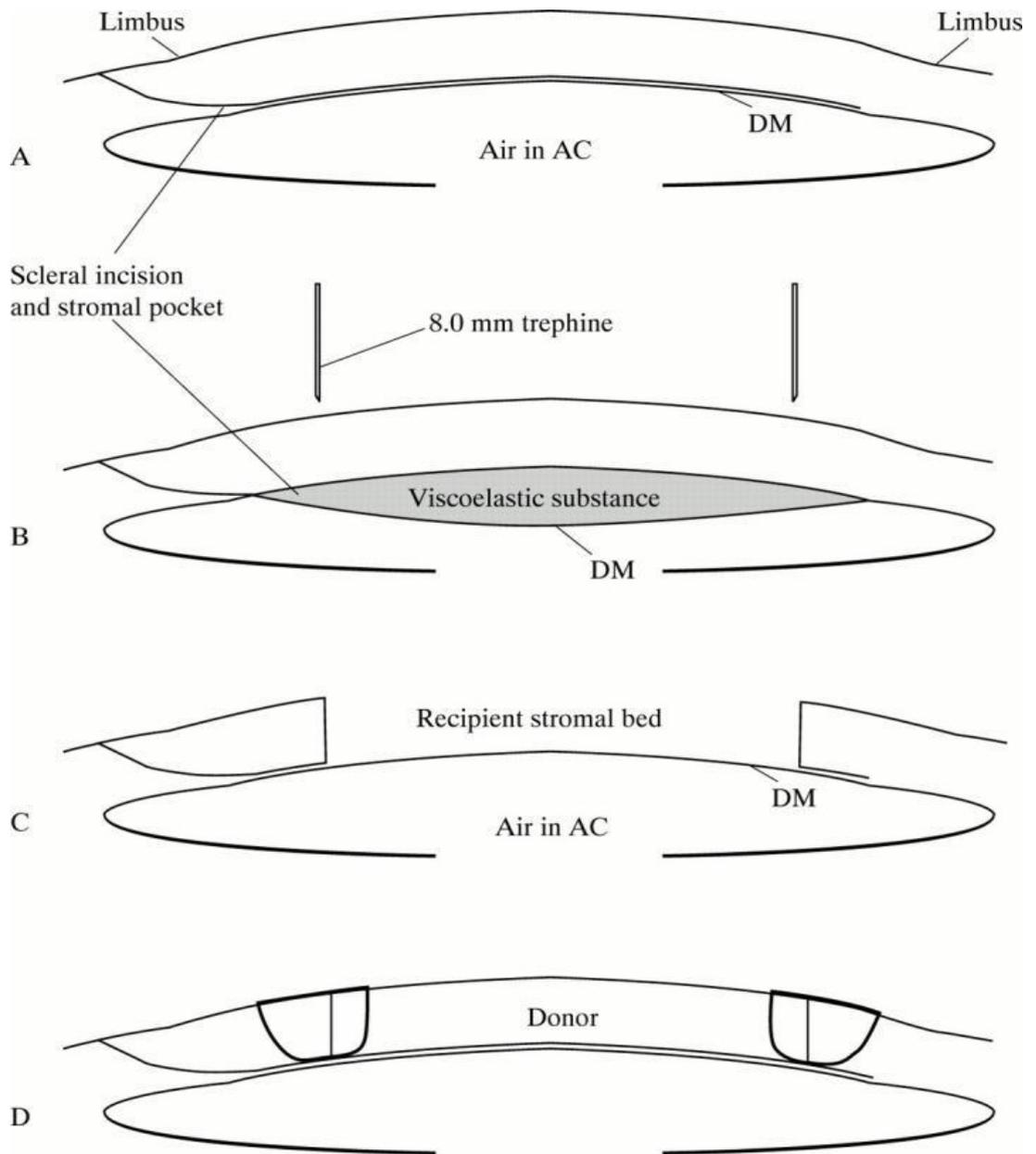
Figure 1.4: Diagrammatic representation of the deep, anterior lamellar keratoplasty technique. (A) After dissection of a deep stromal pocket through a scleral incision. (B and C) Viscoelastic is injected into the pocket, and an anterior corneal lamella is trephinated from the recipient cornea. (D) After stripping Descemet's membrane, a full thickness donor corneal button is sutured into the recipient stromal bed. Compare with Figures 2A-C and 3A-F. Adapted from Melles G et al 1999.

Outcomes:

Many studies have done comparing the PK and DALK outcomes. In terms of best corrected visual acuity (BCVA) and refractive errors both techniques have shown the same outcomes. However, baring the DM or minimisation of residual stroma< 25-65 μm, will improve the visual outcomes in DALK more than PK. But if the residual stroma was thicker or DM wrinkles existed, vision may be less in DALK [20]. Epithelial and stromal rejection occurs in both procedures, but endothelial immune reaction does not occur in DALK. A study conducted by Sari et al found that there was no significant difference in the contrast sensitivity function between PK and DALK patients and this findind was similar to other study compared contrast sensitivity between PK and DALK [21, 24]

Complications of DALK:

The most common complications which are exist after DALK and regarded as a unique to this technique are ruptured DM, large lamellar microperforations, and endothelial cell loss after air injection, interface haze and neovascularisation, wrinkles of the DM and recurrent stromal dystrophy [20].Stromal rejection and/or stromal neovascularisation and Urettes-Zavalia syndrome, where the pupil becomes fixed, dilated and adherent

to the anterior lens capsule due to air injection to the anterior chamber are other serious complications of DALK surgery [24].

1.11 Evolution of Endothelial Keratoplasty

In 1950, Barraquer was the first who describe posterior lamellar keratoplasty in an attempt to treat endothelial pathology. Following that, Terry and Ousley described the deep lamellar keratoplasty in 2001. Further development in EK was introduced by Price Jr and Price in 2005, where they done their first Descemet's stripping endothelial keratoplasty (DSEK). Later on, Gorovoy added automation by using microkeratome for Descemet's stripping to become Descemet's stripping automated endothelial keratoplasty (DSAEK). Melles et al describe the Descemet's membrane endothelial keratoplasty (DMEK) a technique which allowed separation of endothelium-Descemet's membrane (DM) without attached stroma. DMEK offers the best anatomical configuration to the patient [24].

1.11.1 Descemet's stripping automated endothelial keratoplasty /Descemet's stripping endothelial keratoplasty (DSAEK/DSEK):

Descemet's stripping automated endothelial keratoplasty (DSAEK) has become popular procedure of keratoplasty surgery for patients with diseases endothelium and healthy stroma. A layer of donor stroma is transplanted in addition to the Descemet's membrane and endothelium [31]. This technique is suitable for treating several endothelial pathologies such as Fuch's endothelial dystrophy, endothelial cell loss, congenital hereditary endothelial syndrome and iridocorneal endothelial syndrome [24].

Surgical Techniques:

The surgical technique of DSAEK is performed by making 4-5 mm limbal or corneo-scleral incision which is used for insertion of the donor's tissue by forceps or a variety of new inserters such as Busin glide and cystotome. Descemet's stripping of 8 mm diameter is performed with a Sinskey hook and corresponded to 8 mm epithelial trephine marker. The donor tissue can be prepared during the operation or precut by an eye bank. In the precut a microkeratome or a femtosecond laser is used for cutting the donor tissue. The microkeratome cutting depth of 350 μm is adjusted and this will prepare a donor tissue

of 150-200 µm, then the donor tissue is trephined to a size most commonly 8–8.5 µm. the recipient's endothelium and Descemet's membrane is then stripped carefully. Insertion of donor tissue by several methods can be done, such as forceps, suture pull-through and cystosome. Air is then injected carefully into the anterior chamber to hold the donor graft unfolded [24, 32].

Sikder et al described another method of cut that performed to obtain thinner donor graft of 120 µm by using double pass microkeratome technique [33]. Philips et al showed that ultrathin cuts with minimum endothelial cut can be prepared by Ziemer LDV, high frequency and low pulse energy femtosecond laser. However, the stromal surface which results from this technique may not be optimal with this technique [34].
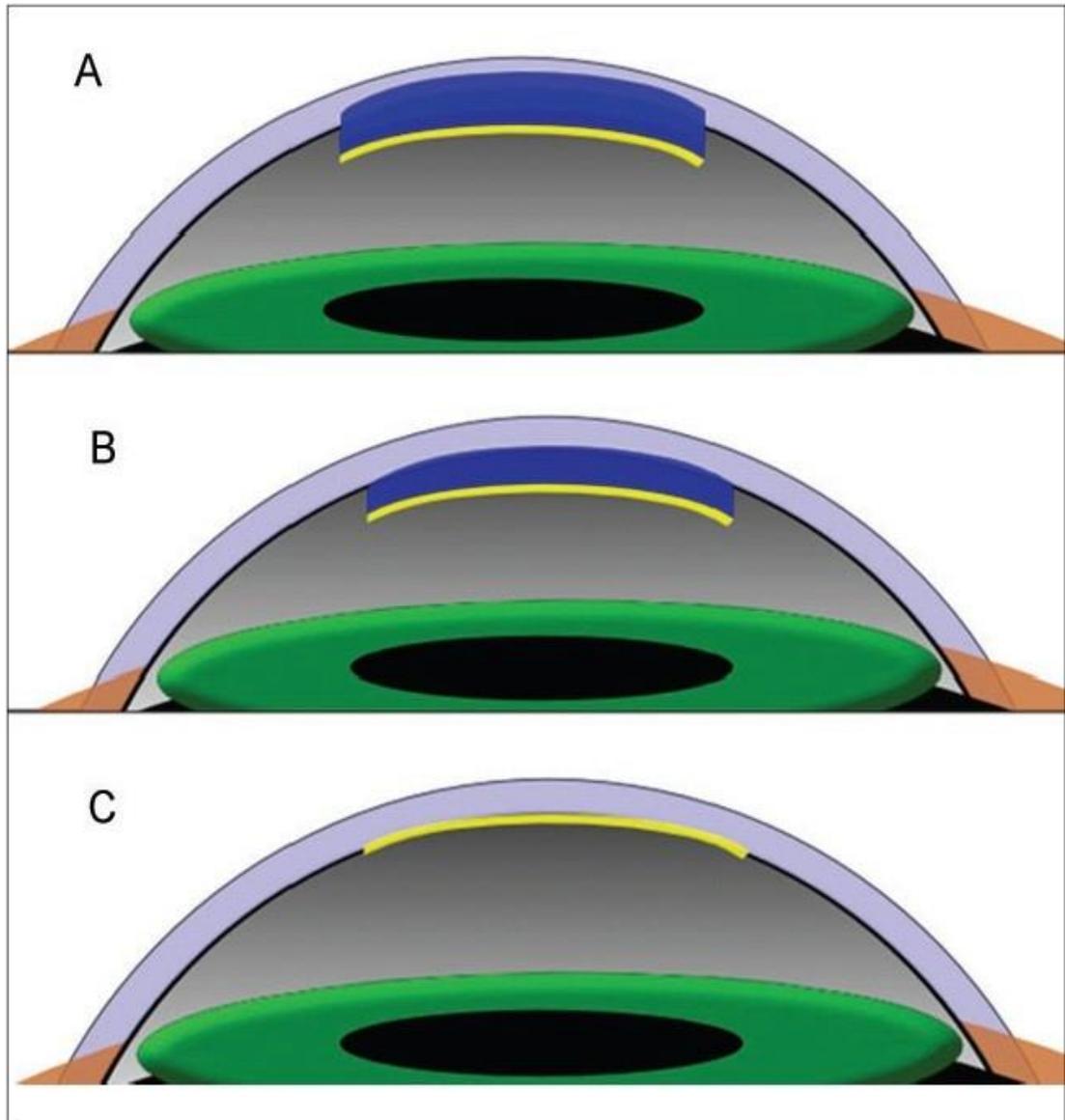
Figure 1.5 **(A) In deep lamellar endothelial keratoplasty, Descemet's membrane and posterior corneal stroma is removed. It is replaced by a graft consisting of posterior stroma and Descemet's membrane; (B) In Descemet's stripping automated endothelial keratoplasty, only the host Descemet's membrane is removed. This is replaced by a donor graft of posterior stroma and Descemet's membrane; (C) In Descemet's membrane endothelial keratoplasty, only the host Descemet's membrane is removed and replaced with the donor Descemet's membrane. Corneal stroma is not transplanted. Adapted from Mark Fernandoz et al 2010.**

Outcomes:

The mean visual acuity after DSAEK is 6/12 if other comorbidities such as glaucoma and retinal disease are excluded. This might be due to the interface light scatter at the tissue interface. Baratz et al found that visual outcomes after DSAEK is also affected by the anterior host cornea, which has more impact on the visual function than the surgical interface [24]. However, Van der Meulen et al has found that donor corneal thickness and stray light have no contributiton to the BCVA outcomes [35].

Complications:

Graft dislocation and primary graft failure are the main complications after DSAEK surgery. The former is considered the most common early complication after DSAEK which requires another bubbling to reattach the graft. Primary graft failure can vary between 0-29% and it is highly correlated with the surgical technique and surgeon's experience [36]. Graft rejection, corneal infection, iatrogenic pupillary block glaucoma and endophthalmitis, all are other complications after DSAEK [24].

1.11.2 Descemet's membrane endothelial keratoplasty / Descemet's membrane automated endothelial keratoplasty (DMEK/DMAEK):

Descemet's membrane endothelial keratoplasty / Descemet's membrane automated endothelial keratoplasty DMEK/DMAEK is a new version of endothelial keratoplasty in which only the DM is transplanted without any donor stroma. DMEK has been named by Melles et al and DMAEK by Price et al [24].

Surgical Technique:

The DM is stripped from the donor cornea directly before the transplantation by the following way: the corneoscleral disc is mounted on a suction trephine. The donor endothelium is marked by 8 mm trephine and stained by 0.06% trypan blue. The central edges of the DM is lifted and then grasped by 2 forceps and detached from the donor cornea. The DM is then detached by centripetal movement of the 2 forceps. The graft is transferred into the recipient's eye by placing the DM in special glass injector such as Melles. Recipient's cornea is prepared by making small limbal incision of about 2.5 mm and the patient's DM is removed using an inverted hook. The donor DM (graft) is then injected into the patient's anterior chamber (AC). Salt solution is then used to centrally position the DM and unfolded by injecting a series of small air bubbles. When the donor graft

is completely unfolded, air is then injected underneath the graft until the AC is totally filled. Air is then left in the anterior chamber for 30 minutes before been aspirated and decreased to around 50% of its AC volume [24, 37].

Outcomes:

Tourtas et al found that Endothelial cell survival six months post-operatively is comparable to that of DSAEK, while DMEK provided faster and complete visual rehabilitation when compared with DSAEK [37].

Rudolph et al compared the outcomes of eyes after DMEK, DSEK, PK and control groups. BCVA was statistically significant and better in DMEK than after DSAEK (P<0.001) and PK (P<0.005). And there was no difference in BCVA between DMEK patients and control groups [38]. They also compared the higher order aberrations (HOA) and found that there was significant difference between DMEK in comparison favourably with PK. However, there was no statistically significant difference between DMEK group and DSAEK and control groups [38].

Providing better visual rehabilitation when compared with DSAEK, Price's group conducted a comparative study on patients whom been operated by DMAEK in one eye and DSAEK in the other eye. They found that BCVA were better in eyes underwent DMEK than those operated by DSEK [39]. Similarly, Melles'

group found that 85% of their study group patients who underwent DMEK have reached equal or better than 20/25 at six months [40].

These studies confirm that DMEK procedure is superior to other types of endothelial keratoplasty in terms of better visual rehabilitation and good post-operative visual acuity.

Complications:

The main post-operative complications are graft rejection and glaucoma.

Price group assessed the relative risk of graft rejection in patients who was undergone DMEK, DSAEK and PK. They found that DMEK patients had a relatively trivial risk of rejection after surgery in comparison with DSEK and PK patients who were undergone surgery for the same indications using similar corticosteroid regimen [41].

Glaucoma is another relatively frequent complication after DMEK that could be eluded by minimising the residual postoperative air bubble to thirty percent in phakic eyes, applying a population-specific steroid regimen, and avoiding decentration of the Descemet graft [42].

1.11.3 Pre-Descemet's endothelial keratoplasty (PDEK):

This is the latest innovation in endothelial keratoplasty and hold considerable promise.

Pre-Descemet's endothelial keratoplasty is a new lamellar corneal transplant procedure in which the donor graft is composed of pre-Descemet's membrane (Dua's layer) with Descemet's membrane and endothelium. This composite is transplanted after taking off the recipient's Descemet's membrane [43]. As it is directly related to one of the aims of the project, details are given in chapter 6.

Surgical Technique:

A corneo-scleral disc is injected with air with the endothelium side up. Injection is done by a 30 gauge needle, and a Type-1 BB created which usually starts from the centre and spreads to the periphery but doesn't reach the extreme periphery of the cornea. The cleaved donor graft is then trephined with a suitable diameter trephine according to the bubble's size. For a smaller size bubble, a suitable size trephine is placed on the central dome-shaped of the Type-1 BB to mark the circumference and trypan blue is injected into the bubble through a peripheral puncture to stain the graft which is then cut rather than trephined. The graft tissue is then loaded into an injector ready

to insert in the recipient's anterior chamber. Recipient's epithelium is marked with trephine of suitable diameter to outline the DM to be excised [43]. The anterior chamber is entered through a corneal tunnel and Descemetorhexis is done with a Sinskey hook, the corresponding DM is then peeled off from the cornea.

The donor tissue is then injected into the anterior chamber; this graft is unrolled using air or fluidics to avoid any contact with the graft endothelium. Although the collagenous property of Dua's layer doesn't overcome the rolling of the graft, it makes the graft roll less tight and the unrolling much easier. When unfolding, an air bubble is injected into the anterior chamber to oppose the graft to the posterior corneal stroma[43] .

1.12 Future Trends and Challenges in Endothelial Keratoplasty Surgery

The desire for better visual outcomes has pushed many surgeons for further development of the endothelial keratoplasty surgery. The achievement of 20/20 vision post DSEAK is usually limited by a variety of causes such as incision induced astigmatism, hyperopic shift caused by transplanted stroma, mismatch between the host and donor corneal curvature and sub-epithelial haze [22].

In contrast, patients who underwent DMEK/DMAEK have better visual outcomes ranging from 20/15 to 20/25. This push advocates of DMEAK/DMEK to prefer these procedures more than DSEK. However, some challenging issues exist such as donor preparation, unfolding the thin tissue, and graft dislocation. Alternatively, some surgeons prefer making a thin cut DSAEK graft so that they can overcome the problems of tissue handling, unfolding and graft dislocation [22].

Endothelial cell loss is another issue of both endothelial and penetrating keratoplasty. Normal endothelial layer is a single layer of approximately 400,000 cells that are 4-6 microns thickness [2]. During the first six months the endothelial cell loss for endothelial keratoplasty is greater than that of penetrating keratoplasty. However, subsequent cell loss is similar. At 5 years later, endothelial loss is more in penetrating keratoplasty than

endothelial keratoplasty (70% vs 53%). Endothelial cell loss can be minimised by using various insertion devices rather than forceps to minimise the trauma that might exist during folding and insertion of donor cornea graft [22].

Nowadays, DSEAK has the predominant form of endothelial keratoplasty. However, if the problems of tissue manipulation and unfolding with DMEAK and DMEK are solved, these procedures could replace DSEK for their confirmed better visual outcomes [22].

1.13 High-risk corneal transplantation

Some corneal grafts are at risk of failure as a results of loss of corneal clarity, poor refractive quality, defective epithelialisation which lead to ulceration and loss of stromal tissue, sever inflammation which end up with tissue degradation. These consequences develop from the drawbacks of the underlying disease or from immune rejection. Patients who are at high risk of graft failure are those with surface disease or underwent corneal transplant due to therapeutic (corneal diseases that is not optical) or tectonic (corneal perforation or thinning) indications. Therapeutic indications are infection such as fungal keratitis, bullous keratopathy to relief pain, and to heal ulcer. Tectonic indications are inflammation such as rheumatoid arthritis and Mooren ulcer, after trauma and infection, and for

corneal thinning (Terrien's marginal degeneration). All these situations have to be carefully managed because it is often associated with sever inflammation, dry eye and lid position disorders [22].

1.13.1 Graft failure due to complications of the underlying disease

There are many causes of transplant failure, including failure to heal such as in anaesthetic corneas such as after herpes zoster ophthalmicus, infection such as fungal and herpes simplex keratitis, epithelial stem cell loss (chemical injuries). Epithelial defect and corneal ulceration are also occure in transplantations in association with allergic eye disease, Rheumatoid arthritis, ocular pemphigoid and Steven-Johnson syndrome [22].

1.13.2 Immunological rejection

The privilege of corneal immunology permits graft transplants free from the risk of rejection, without prophylaxis, in about 80% of the low-risk keratoplasty such as keratoconus. Corneal rejection at the level of epithelium and stroma can be of minor consequences for vision, because rejection can be reversed by the use of topical steroids. Nevertheless, rejection at the level of the corneal endothelium can be of high risk of acute corneal

transplant failure because of the permanent and rapid loss of endothelial cells either immediately or earlier than usual corneal graft failure. The endothelial cells incapable of replication and such loss of less than 500 mm^2 (normally 2500 per mm^2)will lead to graft oedema and loss of corneal clarity[22]. Risk of endothelial rejection grows up to 50% at 5 years if there is recent host corneal inflammation; vascularisation of the recipient corneal stroma and if there is history of previous corneal rejection [22].

1.13.3 Prophylaxis of corneal graft rejection

There is a controversy about the value of tissue matching in the prophylaxis of corneal graft rejection, and its role is unclear [44]. The mainstay prophylaxis of corneal rejection is the topical steroids. Their side effects (cataract and glaucoma) can be easily managed by surgery in case of cataract or anti-glaucoma medicines. Recent studies have shown that long-term use of topical steroids reduces risk of rejection and improve outcomes. A combination of cyclosporine and topical steroids has been ineffective in corneal rejection prophylaxis in many studies including randomised clinical trials [45]. The use of tacrolimus and sirolimus and mycophenolate combination has been reported to have success in few case studies. However, one random study of mycophenolate monotherapy has revealed a positive effect.

On the other hand, the use of systemic immunosuppressive therapy such as systemic cyclosporine, remains to have high quality evidence of success in minimising the risk of corneal rejection [22].

1.14 Optical Coherence Tomography:

Optical Coherence Tomography (OCT) is a fundamental medical diagnostic device which performs micron-scale, cross-sectional, high resolution imaging of the biological tissue by measuring the echo time delay and the intensity of light [46, 47]. OCT is a powerful imaging device because it assists the real time imaging of the anterior segment eye and retina with a resolution of 1 to 15 μm that is finer than the conventional imaging modalities such as ultrasound, magnetic resonance imaging (MRI), or computed tomography (CT). Since its existence in 1991, OCT has been used in a variety of clinical applications in ophthalmology. It is regarded as the standard management in several anterior eye diseases, where it provides a high resolution imaging that was impossible to achieve before the development of the OCT[46].

The first established anterior segment OCT was in 1994 by Izatt et al [48]. The axial resolution was 10μm in tissue, and imaging was done at a wavelength of 800 nm. Later on OCT system for anterior segment uses light at longer than 1300 nm that minimises the scattered optical light and improves the depth of penetration to 21 mm in dimension permitting imaging of the whole anterior chamber. The OCT image reveals the corneal thickness, the curvature of the anterior and posterior surfaces of the cornea and the depth of the anterior chamber [46].

OCT is especially significant in Ophthalmology and in the field of the anterior eye imaging because it offers non-contact, real time, cross-sectional image. This can help to provide a diagnostic Information of the anterior eye enables visualisation of the cornea, anterior chamber, iris and the angle [46].

1.14.1 What an OCT Image Can Show?

OCT image depends on the difference between backreflection and backscattering of the light from the OCT device. Light reaches the deep intraocular tissue undergo transmission, absorption and scattering. Transmitted light can travel into deeper tissues without attenuation. Absorption occurs when light incident chromophores such as, haemoglobin and melanin. Optically scattered light occurs when light transmitted through heterogeneous medium. Backreflection is achieved if the light incident at a boundary between two materials of different refractive indices, such as cornea and aqueous humour. While backscattered light is the light which completely reverses direction when it is scattered [49, 50].

OCT images are composed of single backscattered light which is propagated into biological tissue. Huang D. et al 2010 state that "The strength of the OCT signal from a tissue structure at a given depth is defined by the amount of incident light that is transmitted without absorption or scattering to that depth, is

directly backscattered, and propagates out of the tissue returning to the detector " [49, 50].

1.14.2 Reflectance of Corneal Structure:

Tissue boundaries can be recognised in OCT images depending on the contrast between the reflected signal strength and the backscattered beam. This contrast varies according to the angle of incidence and the tissue of interest. The corneal stroma appears brighter than the epithelium close to the centre, whereas further from the centre the stromal reflection weakens toward the periphery. This is probably due to the angle incidence of the light [49, 50]. The corneal stroma consists of cylindrical collagen fibres which are organised into lamellae; this makes the backscattering light from the stroma a mirror-like. The posterior stroma reveals more directional reflection than the anterior stroma; this might be due to the presence of interweaving fibres in the anterior stroma [50].

1.14.3 Ultrahigh Resolution Optical Coherence Tomography

In vivo ultrahigh resolution OCT provides a resolution of 2-3 μm, this resolution enables visualisation of the intracorneal architecture. This can clearly differentiate the corneal epithelium, bowman's layer and corneal lamellae. However, Descemet's membrane was thought to be difficult to be visualised which may be due to the inadequate contrast between the stroma and the endothelium [51]. However, advancement in OCT technology and development in resolution made it easy to visualise and assess the thickness of Descemet's membrane and Dua's layer (Chapter 5).

1.15 Hypothesis and aims

Human eye bank donor eyes were used to perform the following experiments:

1. Evaluation of endothelial cell counts related to tissue preparation for Pre-Descemet's endothelial keratoplasty (PDEK).

2. Measurement of intra bubble and popping pressure.

3. OCT characterisation of the novel corneal layer named Dua's layer.

4. Further insight in to the microanatomy of the peripheral cornea.

CHAPTER 2

2. GENERIC MATERIALS AND METHODOLOGY:

2.1 Ethics Approval

Ethical approval where obtained from the HRES Committee East Midlands (Nottingham) and the Research and development of the National Health Service trust. Correspondence Research Ethics Committees reference No. 06/Q2403/46.

2.2 Principle

The use of the human Sclero-corneal tissue for Sclero-corneal discs were kept in organ culture in Eagle's minimum essential medium with 2% foetal bovine serum for four to eight weeks post-mortem.

Air injection was performed on human sclera-corneal discs and it was noted to spread from the site of injection, circumferentially and posteriorly to fill the corneal stroma and eventually result on the formation of a Big Bubble.

2.3 Evaluation of endothelial cell counts related to tissue preparation for Pre-Descemet's endothelial keratoplasty (PDEK).

Tissues were harvested from 10 eye bank sclera-corneal discs by trephination after air injection into corneal stroma and BB formation. Five corneas were allocated for each type; PDEK tissue samples were prepared from T1BB and DMEK from T2BB. Another five samples for each group were used as controls. Endothelial cells were counted and compared before and after injection using phase-contrast microscopy with an eye piece reticle. Paired t test was used to analyse the results.

2.4 Optical Coherence Tomography (OCT)

In this study, I used both Topcon and Spectralis OCT (Optic Coherence Tomography) to image type 1 big bubble (T1BB), Type 2 (T2BB), Mixed BB, and T1BB with Descemets membrane (DM) peeled. The definition of the different layers of the BB was clearer in Spectralis than in Topcon OCT. We have also collaborated with the University of British Colombia, Vancouver and carried out Visante (time domain) OCT on the BB to obtain wide angle images of the wall of the BBs.

2.5 Measurement of Intrabubble and Popping Pressure and Bubble volume

In this part of our study, we are ascertain the strength of the wall of TI BB (Dua's layer) and T2BB (DM) by measuring the pressure required for both T1BB and T2BB to burst. A customised digital pressure gauge to continuously record in real time the injection pressure was constructed with the help of the Medical Physics department and use of commercially available hardware and software (See figure 3.1). Also, we have measured the amount of air in the bubble and the compression volume or air required to create the bubble. During the experiments, we created the BB by air injection in the corneal stroma of cadaver, eye bank corneoscleral discs. The needle was advanced into the BB and the pressure increased until bursting point of the BB. The pressure was digitally recorded.

2.6 Further insight in to the microanatomy of the peripheral cornea.

We conducted experiments wherein at the initiation of a T2BB we stopped injection of air and peeled off the DM and subjected the stroma under the DM to scanning electron microscopy

(SEM). Control samples without air injection and from which the DM was removed were also studied.

CHAPTER 3

Air pressure changes in the creation and bursting of the type-1 big bubble in deep anterior lamellar keratoplasty: an ex-vivo study.

3.1 Introduction

Deep anterior lamellar keratoplasty (DALK) has replaced penetrating keratoplasty as the procedure of choice in surgical management of eyes with diseases affecting the corneal stroma and affecting sight such as scars, dystrophy or ectasia. The Big Bubble (BB) technique [28] is the most popular technique wherein air is injected in the corneal stroma to separate either the Descemet's membrane (DM) or the DM together with a layer of deep corneal stroma termed the pre-Descemet's layer (Dua's layer–DL). This allows excision of the affected stroma and recipient epithelium and replacement with healthy stroma and epithelium from a cadaver donor.

When air is injected in the corneal stroma either cleaves the DL from the deep stroma to create a big bubble termed type-1 or it accesses the plane between DM and DL to create a thin walled bubble termed type-2. The wall of a type-1 BB is made of DL and DM while of a type-2 BB is made of DM alone and is more vulnerable to major tears or bursting during surgery. Often

during injection of air, tiny bubbles escape from the peripheral cornea, in the vicinity of the trabecular meshwork in to the anterior chamber and can cause post-operative raised intraocular pressure [22, 24, 52].

Dua et al have reported that DL is a strong and resilient layer with bursting pressure 1.45 bars [4]. Based on the above information, Zaki AA et al described a combination of DALK with phacoemulsification and lens implant, termed the DALK-Triple procedure. When confronted with patients requiring DALK who also had dense cataracts they were able to perform cataract surgery under the exposed DL of a type-1 BB. They reported that DL could withstand all pressure fluctuations associated with the phacoemulsification procedure and that despite stromal scarring requiring keratoplasty, the DL was remarkably clear in most cases [14]. In one instance they attempted DALK-Triple under the DM (type-2 BB), which burst promptly during injection of viscoelastic in the anterior chamber.

In this study we report the pressure and volume of air required to create the BB, the volume and pressure of air in the type-1 BB and the bursting pressure of the type-1 BB.

3.2 Materials and Methods

3.2.1 Tissue samples

Twenty two human sclero-corneal discs from eye bank donor eyes that were not suitable for transplantation were used. The sclera-corneal discs were maintained in organ culture in Eagle's minimum essential medium with 2% foetal bovine serum for four to eight weeks post-mortem. Donor details are given in table 3.1.

Table 3.1 Donor details for the sclera-corneal discs used in the experiments.

Sample No.	Type of big bubble (BB)	Sex	Age	Date of death	Cause of death
E1955	T1BB	F	67	08/05/2014	Stroke
E2168	T1BB	F	60	29/12/2014	Other (unknown)
E2182	T1BB	F	58	07/01/2015	Cancer
E2183	T1BB	F	58	07/01/2015	Cancer
E2246	T1BB	F	69	15/03/2015	Chronic obstructive pulmonary disease
E2187	T1BB	F	65	02/01/2015	Pending
E2385	T1BB	M	73	29/06/2015	Respiratory failure
E2347	T1BB	F	52	17/06/2015	Encephalopathy
E2278	T1BB	F	80	07/05/2015	sepsis
E2276	T1BB	M	74	01/05/2015	Brain damage hypoxia

E2275	T1BB	M	74	01/05/2015	Brain damage hypoxia
E2309	T1BB	M	72	02/04/2015	Cronic obstructive pulmonary disease
E2326	T2BB	F	75	04/05/2015	Myocardial infarction
E2348	T2BB	F	52	17/06/2015	Encephalopathy
E2384	T2BB	F	68	14/07/2015	Myocardial infarction
E2677	T1BB	F	81	29/12/2015	Myocardial infarction
E2675	T1BB	M	53	02/01/2016	Unknown
E2674	T1BB	M	53	02/01/2016	Unknown
E2678	T1BB	F	44	14/12/2015	Intracranial heamorrhage
E2679	T1BB	F	44	14/12/2015	Intracranial heamorrhage
E2829	T1BB	M	80	14/03/2016	Cancer
E2836	T1BB	F	88	03/04/2016	Old Age

3.2.2 Experiment to measure pressure

3.2.2.1 Air injection

The sclero-corneal disc was placed endothelial side up in a petri dish and kept moist with balanced salt solution. In fifteen samples, under an operating microscope, a 30 gauge needle, bent to an angle of 135 degrees, bevel up, attached to a 20 ml syringe was passed from the scleral rim into the corneal stroma and advanced to the centre of the disc. The needle was passed close to the endothelial surface without perforating it. Air was injected with force to overcome the tissue resistance, until a big bubble was formed. The type of the bubble was determined, type-1 or type-2. The position of the needle tip was kept constant in the centre of the sclera-corneal disc in mid stroma.

3.2.2.2 Pressure measurement

An electronic pressure gauge/converter device was used (Keller, K-114, Winterthur, Switzerland). The tube from the device was linked to the side arm of a 3-way cannula attached between the syringe and needle. The injecting needle was attached to the front end of the cannula and a 20 ml syringe to the other end. The device was also connected to a personal computer (PC) via a USB port. The USB link also powered the device. Pressure readings were recorded in real time and transmitted as serial

RS485 half-duplex signals to the PC where the pressure was displayed as a continuous trace on the screen by the software associated with the K-114 device. (Figure 3.1) The pressure recorded was that in the syringe during injection of air. In validation experiments, when the needle was not inserted in tissue and the piston was advanced rapidly, the pressure recorded was between 0 and 1, indicating that the resistance offered by the needle was not relevant to the pressures measured (data not shown).
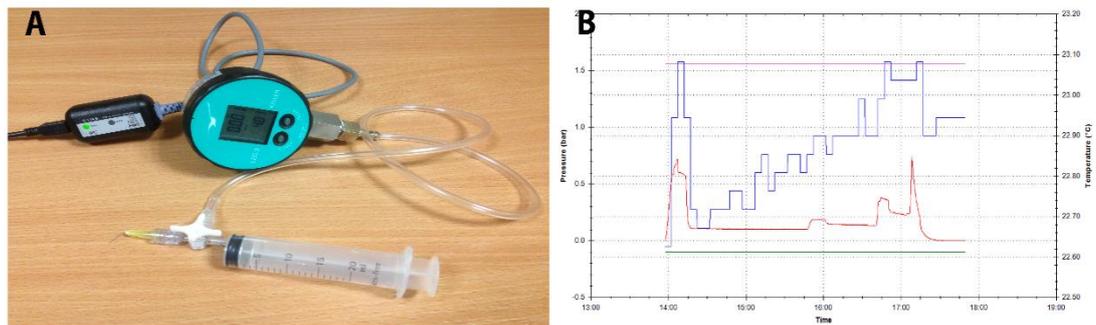
Figure 3.1 (a) Pressure converter system K-144, (b) Real pressure record over time (red graph), the temperature of the pressure sensor (blue graph), the maximum pressure (pink graph), the minus pressure (green line).

The maximum pressure required to create the bubble was recorded. The plunger was then released and allowed to attain a stable position. The needle tip was advanced to lie inside the BB and the bubble inflated till its wall was taut. The pressure recorded at this point was taken as the base line intra-bubble pressure. With the needle tip in the BB, the piston was pushed

further with force until the BB burst. This recorded the bursting pressure of the bubble (Figure 3.2 a, b).
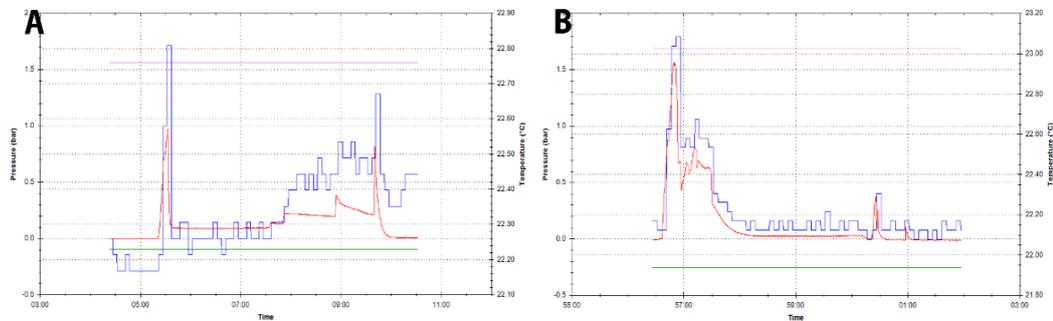
Figure 3.2 (a) pressure change over time (red line) in T1BB. (b) Pressure change over time (red line) in T2BB.

3.2.3 Experiment to measure Volume

As air leaked through multiple points along the circumference of the corneal periphery a clamp was designed to block the holes and stop air leak. In 7 samples, the sclero-corneal discs were clamped in a circular clamp of 10mm diameter that prevented air escape from the periphery. A 30 gauge needle attached to a one millilitre syringe (internal diameter 5 mm) filled with air was passed in to the corneal stroma from the scleral rim as described above. During injection the maximum compression of air (position of piston) at the time air just started to appear in the corneal stroma was recorded. The piston was held in place until a type-1 BB was formed. The pressure on the piston was released and piston allowed to reverse to a stable position. The

volume of air lost in the cornea was ascertained from the final position of the piston. The BB diameter was measured with a pair of surgical callipers. The needle was then advanced into the BB and all the air aspirated until the BB had completely collapsed. This provided a measure of the volume of air in the big bubble. The pressure (above atmosphere) in the syringe at the point where air started to emerge in the tissue from the needle tip was deduced by the formula $P1V1 = P2V2$, where P1 is the initial pressure (atmospheric) and V1 the initial volume (1ml) and P2 is the final pressure (unknown) and V2 the final volume (mean 0.54ml, see results).

3.3 Results:

The average age of donors was 66 years (range; 52-80 years). There were 15 females and 7 males.

3.3.1 Pressure measurements

Twelve type-1 and 3 type-2 BB were obtained (table 2). The mean pressure attained to create a BB was 96.25+/- 21.61 kilopascal (kpa) (range 90-130kpa). For type-1 BB the mean intra-bubble pressure was 10.16 +/- 3.65kpa (range 5.2-18kpa) and the bursting pressure was 66.65 +/- 18.65kpa (range 40-110kpa). The median bursting pressure was 68.5kpa (table 3.2). Accurate measurements of type-2 BB could not be obtained as

when advancing the needle into the bubble cavity, while the needle was still in the stroma, the type-2 BB burst in one case and the DM disinserted (separated along its peripheral attachment to the stroma) in one sector before the bubble could be inflated enough to make the DM taut. The mean pressure at the time the type-2 BB burst/disinserted was 14.77 +/- 2.44kpa (range 12.0-17.0kpa) (table 3.2).

Table 3. 2 Measurements of the big bubble.

	Sample No.	Diameter(mm)	Intrabubble pressure(Kpa)	Bursting pressure(kpa)
T1BB	E1955	nm	nm	45
	E2168	7	12	60
	E2182	9	13	80
	E2183	8.5	14	73
	E2246	8.5	11.6	66
	E2187	8.5	18	40
	E2309	8.5	7.5	110
	E2275	8.5	7.5	78
	E2276	8.5	7.5	55
	E2278	nm	5.2	71
	E2347	8.5	6.8	76.8
	E2385	8.5	8.7	45
T2BB	E2326	10	nm	17
	E2348	10.5	nm	12
	E2384	10.5	nm	12.7

3.3.2 Volume measurements

In the bubble volume experiment, the maximum compression of air required to create type-1 BB was 0.54 +/- 0.07 ml (range 0.5-0.7 ml), the volume of air lost in the cornea was 0.38 +/- 0.06 ml (range 0.3- 0.5 ml) and the average volume of the BB was 0.1 ml.

The mean pressure in the syringe at which air started to emerge in the tissue, as calculated from the volume compression, was 131.82+/- 50.58kpa (range 101.28 – 236.3 kpa above atmosphere) (Table 3.3).

Table 3. 3 Bubble volume measurements.

Sample Number	Max compression (ml)	Pressure in the syringe (kpa)	volume of air lost in cornea (ml)	Amount of air sucked (ml)	Bubble diameter (mm)
E2677	0.5	101.28	0.41	0.1	7.5
E2675	0.5	101.28	0.3	0.1	7.5
E2674	0.5	101.28	0.4	0.1	6.5
E2678	0.7	236.3	0.5	0.11	7.5
E2679	0.64	180.08	0.43	0.1	7.5
E2829	0.5	101.28	0.36	0.1	7.5
E2836	0.5	101.28	0.3	0.1	7.5

The pressures measured directly with the gauge and by this method was not statistically significant (p= 0.25) (Figure 3.3).

Statistical methods: The data was normally distributed as confirmed by Levene's test. Statistical analysis between two groups was performed by the unpaired student t-test using Graphpad prism version 5.0. (Graphpad software, USA). p<0.05 was considered statistically significant."
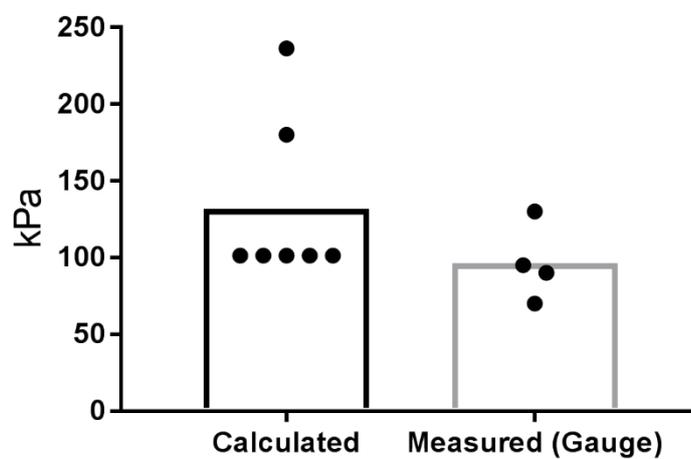
Figure 3.3 Compares the pressure calculated from the volume compression of the syringe and that measured directly with gauge (p= 0.25).

3.4 Discussion:

In DALK by the BB technique, when air is injected in the corneal stroma, a type-1 BB forms by air cleaving in the plane of deep stroma and DL, with a posterior displacement of DL and DM. The cleavage and displacement are related to the pressure of air in the corneal stroma and in the BB. As the BB expands posteriorly the intra bubble pressure is countered by the intraocular

pressure, which can rise to 70 mm of mercury (authors' unpublished observations). This counter pressure and the closed space within which the BB expands limits the posterior expansion of the BB in the eye thus rupture of a type-1BB during inflation is unlikely and has not been reported. However, when the type-1BB is deflated and the corneal stroma anterior to it is removed, the DL + DM bulge anteriorly to assume a convex dome shape. Any pressure applied to the DL+DM from within the eye, as during the DALK-triple procedure, would cause the layers to expand outward, into the atmosphere and theoretically reach a bursting point. In this study I set out to ascertain the minimum and mean popping (bursting) pressure of the layers to establish whether it would always be safe to perform cataract surgery under DL+DM after creating a type-1BB.

The pressure converter K 114 allowed us to measure in real time the pressure at the tip of the needle during the creation of a BB. On initiation of injection, air is compressed in the syringe on account of the tissue resistance offered by the corneal stroma at the site of the tip of the needle. Once this is overcome, air starts to enter the stroma separating the lamellae and the intrastromal pressure builds up as the cornea gets completely aerated. At a critical tissue pressure, the air forces its way to the plane anterior to DL and cleaves this away from deep stroma as a

type-1BB. The volume of air required to achieve the critical tissue pressure depends on the escape of air through the trabecular meshwork or through distinct peripheral holes in the stroma, during injection [43, 53]. This confounder was eliminated by the use of the clamp, which prevented any escape of air thus giving us an accurate measure of the mean tissue pressure required to create a BB overcoming tissue resistance, which was 96.25 +/- 21.61 kpa. It has been recently demonstrated that air injected in the corneal stroma follows a consistent path regardless of the location, direction of bevel and depth of the needle tip in the stroma [54]

Once a type-1BB was created the intra-bubble pressure was ascertained by advancing the needle into the cavity of the BB. This measured 10.16 +/- 3.65 kpa. In the ex-vivo situation of this study, it was possible to expand the type-1BB to its bursting point by continued forceful injection of air with the needle positioned in the cavity of the bubble. This situation would simulate increased intraocular pressure exerted on the layers during phacoemulsification carried out under the layers (DALK-triple). The lowest pressure at which a type-1BB burst was 40 kpa and the highest was 110 kpa. The mean bursting pressure was 66.65 +/- 18.65 kpa. Although Dua et al reported the bursting pressure in the original paper [4], I refined the measurement by placing the needle tip in the type-1 BB while

increasing the pressure to bursting point. This approach eliminated any variations induced by the resistance of the stroma to the passage of air. Any effect of variable leakage of air from the periphery of the sclera-corneal was prevented by the use of the clamp. In addition, the accuracy of the measurements was enhanced by using the continuous digital pressure recording device.

A number of studies have reported the variations in intraocular pressure during phacoemulsification. By direct measurements during surgery Zhao Y et al found that the IOP fluctuated from 13-96 mm Hg (1.8-13.5 kpa) [55]. Khng C et al state that IOP exceeded 60 mm Hg (8.4 kpa) and the highest IOP occurred during hydro-dissection, viscoelastic injection and intraocular lens insertion [56]. Vasavada V et al compared the impact of different fluidic parameters on intraoperative IOP and found that the minimum IOP in the low and high parameters groups was 35 mm Hg (4.9 kpa) and 34.5 mm Hg (4.8 kpa) respectively, and the maximum IOP in the low and high parameters groups was 69 (9.7 kpa) and 85 (11.9 kpa) mm Hg respectively [57]. In another study Kamae KK et al monitored IOP during IOL implantation and found that the mean and peak IOPs exceeded 60 mm Hg (8.4 kpa) during IOL implantation [58]. In comparison, the data on bursting pressure of the DL+DM generated in this study show that the pressures attained during

cataract surgery are several times less than what is required to burst the layers under which phacoemulsification can be carried out in the DALK-triple procedure. Even the lowest bursting pressure had a safety margin of over 25 kpa (177.5 mm Hg) compared to the highest pressure reached during phacoemulsification. This would indicate that DALK-triple is a viable option with regard to the risk of inadvertent rupture of the DL+DM layers intraoperatively.

When cataract and DALK surgery are required simultaneously; if the cornea is clear, one could consider performing phacoemulsificaton as the first step and DALK as the second step of the same procedure. However, when the cornea is scarred to an extent that visualisation is poor, a triple-DALK would be the preferred option. With triple-DALK, when air injection fails to produce a type-1BB, manual dissection allows access to the plane between the deep stroma and DL. Once the opaque cornea, related to the aeration of the stroma anterior the DL is removed, the transparent DL allows phacoemusification to be carried   out.

I was able to create both type-1 and type-2BB as reported by Dua et al 2013. However, the type-1BB was more consistent occurring in 86.4% of the 22 sclero-corneal discs. The data

provided in this study can help to develop an automated system whereby we can produce big bubbles in vivo with improved consistency.

CAPTER 4

DYNAMICS OF BIG BUBBLE FORMATION IN DEEP ANTERIOR LAMELLAR KERATOPLASTY (DALK) BY THE BIG BUBBLE TECHNIQUE: IN VITRO STUDIES.

(This work has been jointly done with another fellow from Cairo University).

4.1 Introduction

Lamellar keratoplasty in the form of endothelial keratoplasty (EK) for endothelial disorders and deep anterior lamellar keratoplasty (DALK) for stromal disorders, has replaced penetrating keratoplasty (PK) as the procedure of choice for several indications [20, 28, 59] For DALK, the big bubble (BB) technique[28], wherein air is injected in the corneal stroma to separate the pre-Descemets layer (Dua's layer, PDL) or the Descemets membrane (DM) from the posterior stroma, is the popular procedure [8, 60, 61]. With pneumo-dissection the type-1BB (cleavage between PDL and stroma) is common but often a type-2BB (cleavage between DM and PDL) or a mixed BB forms [4, 62]. Injected air traverses the thickness of the stroma and on reaching the posterior lamellae, lifts off the PDL, which is impervious to air [4, 62]. Very little is known of the path air traverses in the stroma before it reaches the respective planes to create a type-1, type-2 or mixed BB. I hypothesized that the

path taken by injected air is determined by the corneal stromal microarchitecture, which influences the type of BB formation. In this study, I examined the movement of air injected in the stroma of human sclero-corneal discs to understand the dynamics of BB formation in the context of the corneal stromal architecture and microanatomy of the posterior cornea. I present evidence to explain the mechanisms of formation of the different types of BB.

4.2 Materials and Methods

Fifty seven human eye bank sclero-corneal discs preserved in Eagle's organ culture medium for up to 10 weeks and 2 fresh sclero-corneal discs were used. The causes of death were infections (n = 10), cardiac related (n = 9), cancer (n = 7), neurological (n= 6) and others (n = 27). Donor age was 55 to 81 with a mean of 66 years. All tissue was from consented donors and released for research by the National Health Service Blood and Transplant Service UK.

4.2.1 Air Injection

In 57 discs intrastromal injection of air was made with a 30-gauge needle attached to a 5ml syringe. The needle bevel was directed to the endothelium in 46 eyes, the epithelium in 5 eyes

and faced sideways in 6 eyes. The characteristics and direction of movement of air from the point of injection to the formation of a BB was captured on digital video. A few drops of balanced salt solution were placed in the concavity of the disc so that any leaking air could be visualised as a string of tiny bubbles. (Figure 4.1 A, B). Leaking points were marked.

4.2.2 Experiment to determine origin of type-2BB

In 5 corneas, when a type-2BB started forming peripherally near the limbus the site was marked. The Descemet's membrane adjacent to the marked point representing the commencement of the type-2BB was peeled off to expose the underlying stroma. This area was examined by scanning-electron-microscopy (SEM). Two fresh sclera-corneal discs without air injection were used as controls. In these two, the Descemet's membrane was completely peeled off and the tissue fixed in glutaraldehyde and processed for SEM.

4.2.3 Experiment to examine characteristics of air spaces within the corneal stroma following air injection

Six sclero-corneal discs were injected with air as described above. In three corneas air injection was ceased when air had

spread along the circumference of the cornea as a narrow band (see results); and in three others air injection was ceased as soon as a type-1BB started to form by the coalescence of smaller bubbles. Samples were fixed for histological examination in 10% formalin for light microscopy and in 2.5% glutaraldehyde for SEM.

4.2.4 Scanning electron microscopy

Samples were treated with 1% osmium tetroxide before dehydrating in ascending grades of alcohol. Samples were then critically point-dried and sputter coated with gold before examination in a JSM 840 SEM (JEOL, Herts, UK) as described previously [4]. The periphery was examined for the presence and distribution of fenestrations.

4.2.5 Light microscopy

Paraffin embedded, 5-micron limbus to limbus sections were cut, deparaffinised and stained with Harris haematoxylin and eosin using standard protocols. Entire sections were scanned with the Nanozoomer 2.0-HT Digital Slide Scanner, C9600, at x 20 magnification. (Nanozoomer Digital Pathology (NDP) System,

Hamamatsu, Japan and the distribution of intrastromal bubbles examined.

4.3 Results

4.3.1 Immediate passage of air

When air emerged at the tip of the needle in the corneal stroma, three patterns were seen.

1. An immediate whitening of the aerated stroma with air and rapid extension in a radial manner to the limbus like the spoke(s) of a wheel numbering 1 to 7 (mean = 2.4) (Figure 4.1 C). This was the commonest pattern seen, in 41/57 samples.

2. Very fine linear branching lines, like 'cracks in glass' appeared from the tip of the needle in 6 samples (Figure 4.1D). The subsequent pattern was as described in (1) above.

3. Air spread diffusely from the needle tip to the periphery in 10 samples (Figure 4.1E). Although the movement of air followed the above three patterns at the earliest exit from the needle tip, a combination of two or all three was seen by the time the whole cornea was aerated (Figure 4.1F).
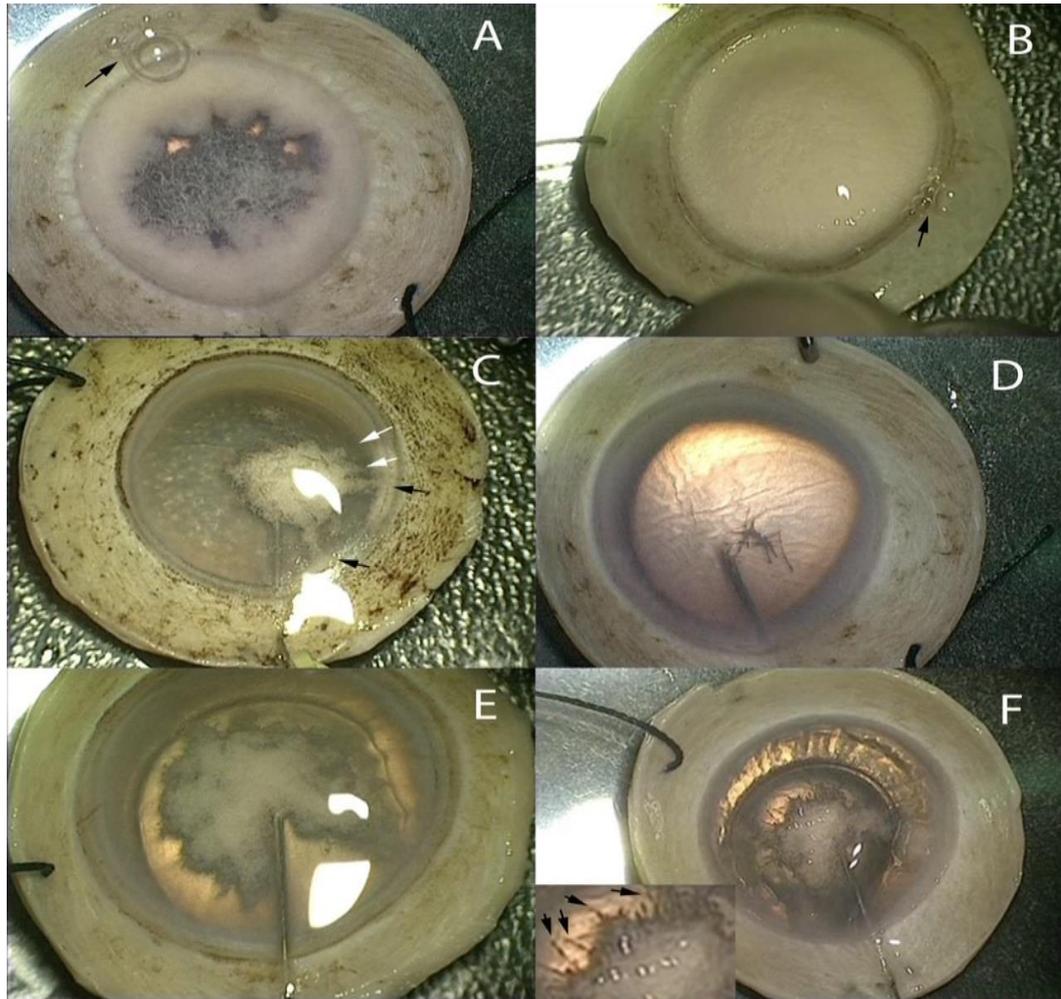
Figure 4.1 Leakage of air at the vicinity of the trabecular meshwork. Sclera-corneal discs are partially (A) and fully (B) aerated. Small bubbles of air are seen to escape at the vicinity of the trabecular meshwork (arrows). Immediate path taken by air injected in the corneal stroma. C. Four radial tracks of air are seen extending from point of injection towards the corneal periphery. Two (black arrows) have reached the periphery and two (white arrows) are mid-way to periphery. D. Fine lines related to movement of air in the stroma, like 'cracked glass' are seen to emanate from the tip of the needle. E. Diffuse centrifugal spread of air in the corneal stroma is seen from the needle tip extending towards the limbus. The aerated stroma appears white. F. A combination of diffuse spread with fine needle-like lines, which are clearly seen at the outer edge of the aerated stroma (inset).

4.3.2 Late passage of air

When one or more spoke(s) of the radially tracking air reached the limbus the direction of air travel changed from radial to circumferential, with the air tracking in both clockwise and counter-clockwise directions along the circumference of the peripheral cornea till the bands met (Figure 4.2) The width of the circumferential band of air was between 1.5 to 2mm. This was the most consistent pattern regardless of the pattern of initial passage of air. Air then moved centripetally from the periphery till the whole cornea became white. On continued injection of air, the cornea expanded in the antero-posterior direction with the posterior, central 6 to 8.5 mm zone expanding the most. The circumferential band remained comparatively more compact than the central cornea (Figure 4.2). There was a ring of constriction (least expansion) between the circumferential band and the central zone (Figure 4.3). During the passage of air, leaking points evident as tiny bubbles of air streaming from specific foci along the circumference of the peripheral cornea, anterior (central) to the trabecular meshwork and from the perilimbal sclera, posterior to the trabecular meshwork also appeared in 52/57 samples. There were 0 to 8 leaking points (mean 4.2) in any given sample (Figure 4.1 A,B). The above patterns of early and late passage of air was observed regardless

of the direction of the tip of the needle whether facing the

epithelium, the endothelium or the limbus.
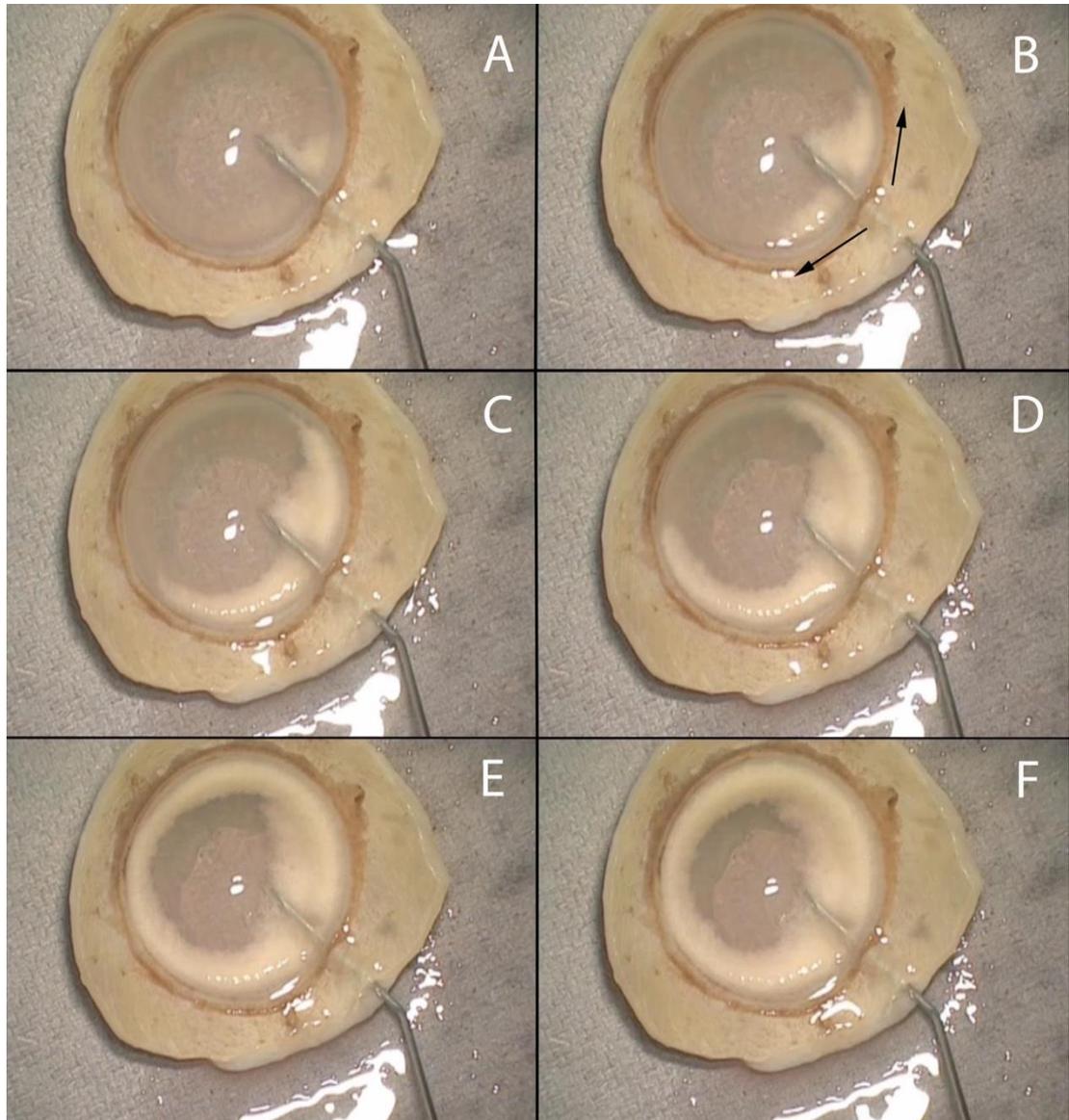
Figure 4.2 Late passage of air: A. A single radial track is seen to extend from the needle tip back towards the limbus. B. On reaching the limbus, air starts to spread circumferentially in both clockwise and counter-clockwise directions (black arrows). C and D. The circumferential movement of air along the limbus is seen as a white band moving in the clockwise and counter-clockwise directions. E. The circumferentially moving bands of air meet each other to complete the circle. F. Further injection results in slight widening and thickening of the band. The central cornea remains clear (unaerated).
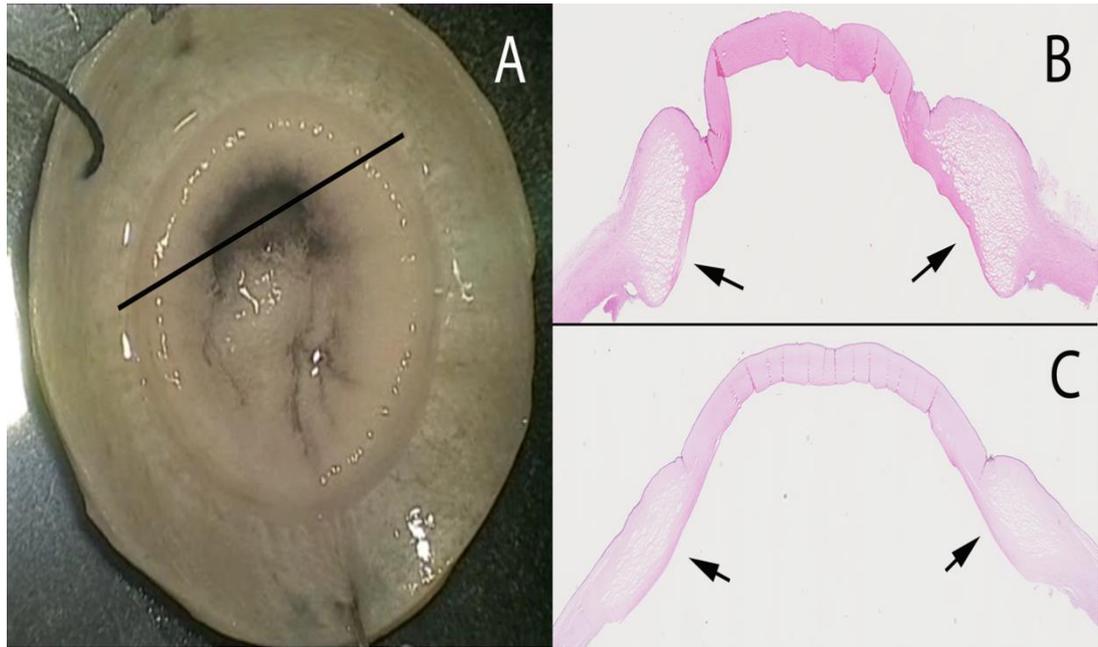
Figure 4.3 Histology of cornea with circumferential band of air. A. A circumferential band was formed after initial diffuse spread of air in the stroma. The thickness of the band can be appreciated by the reflection of light as tiny dots from the convex surface of the band, seen as a circle inside the limbus. The black line represents the plane of the histology section. B and C. Hematoxylin and eosin stained sections of two corneas where the circumferential band was complete and the central cornea was clear (unaerated). The peripheral corneal stroma corresponding to the circumferential band (arrows) shows many intrastromal pockets of air, separating the collagen lamellae. The aerated area is lined anteriorly and posteriorly with compact unaerated stroma.

Three further patterns emerged in the 51 samples where air was injected until a complete big bubble was formed:

1. Type-1BB: Tiny bubbles appeared anterior to the Descemet's membrane and coalesced to form a big bubble that lifted the posterior wall of the type-1BB like a dome, which expanded to a mean width of 8.5 mm (range 7 to 9mm) (Figure 4.4 A-D). The circumference of the type-1BB corresponded to the inner circumference of the circular band air at the periphery. The type-1BB was observed in 35/51 samples.

2. Type-2BB: A thin walled bubble appeared at the periphery and expanded as a thin transparent dome across the surface of the cornea measuring 10 mm to 10.5mm in diameter representing a type-2BB in 9/51 samples (Figure 4.4 E,F).

3. Mixed BB: In 7/51 samples both type-1 and a type-2BB developed together. In 5 samples the type-1BB was complete but the type-2BB was partial and in 2 samples both type-1 and type-2BB were complete (Figure 4.4 G,H). In 2 samples it was noted that the type-2BB started at the edge of a type-1BB after the type-1BB had reached its maximum diameter while in the remaining 5 it started at the periphery as described in '2' above.
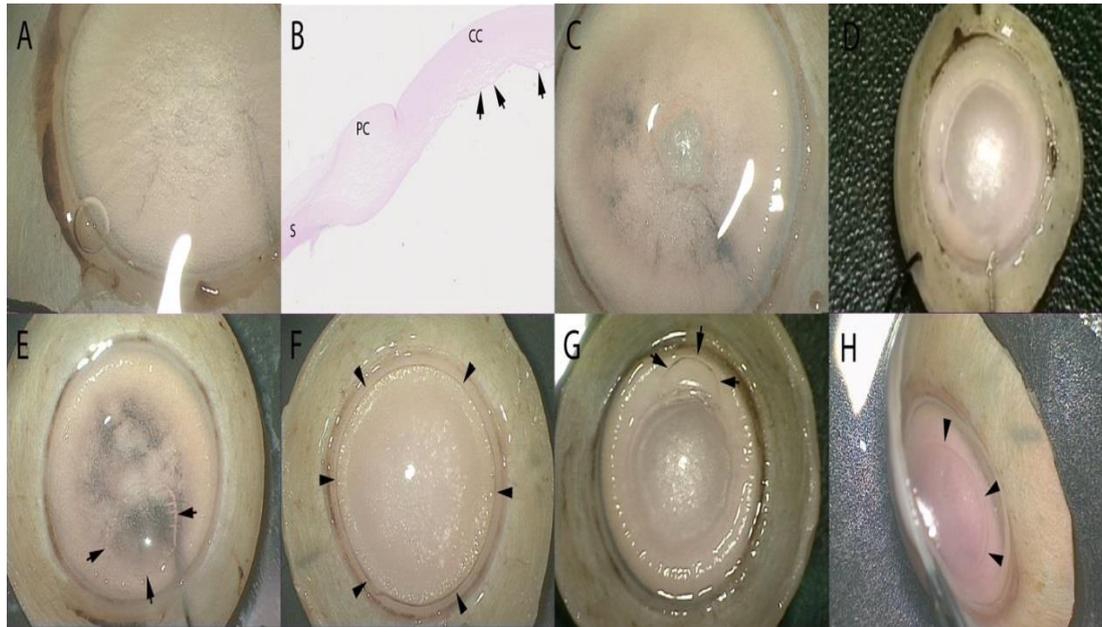
Figure 4.4 Formation of type-1 big bubble (BB). A. A cluster of tiny bubbles of air are seen in the central corneal stroma, which is fully aerated and appears white. B. Hematoxylin and eosin stained section through the cluster. The sclera (S) is compact. The peripheral cornea (PC) shows the circumferential band as in Figure 4.3. Air is seen to spread from the peripheral band to the center (CC) in the deep stroma. The central cluster is seen to be made of multiple small pockets of air lying just posterior to the Descemets membrane and the pre-Descemets layer (Dua's layer). C. The tiny bubbles/pockets of air have coalesced and the commencement of a type-1BB is clearly visible in the center of the cornea. D. The type-1BB is fully formed. The circumference of the type-1BB corresponds to the inner circumference of the circular band of air at the periphery. Formation of type-2 big bubble (BB). E. The commencement of a type-2BB is seen as a small thin-walled bubble at the periphery of the cornea. The margin of the bubble is indicated by the black arrows. F. A complete thin-walled type-2BB, which extends across almost the entire surface of the cornea is seen. The outline of the BB is indicated by the arrowheads. This extends up to the outer circumference of the circular band at the periphery. G. Mixed BB. A centrally located type-1BB is seen with small incomplete type-2BB (black arrows) located at the periphery of the cornea. D. Mixed BB. A complete type-1BB (black arrowheads) is seen encased in a larger thin walled type-2BB (white arrows).(representative photo from approximately 10 samples).

4.3.3 Electron microscopy

On SEM, tiny holes were seen in the peripheral cornea adjacent to the origin of the trabecular meshwork corresponding to the leaking points of air. In the 5 samples where the start of the type-2BB was marked and the DM peeled off prior to SEM, clusters of fenestrations were noted in the PDL, within 500 microns central to the termination of DM. In the two fresh samples that were not injected with air, 15 and 20 clusters of

fenestrations were found respectively, along the circumference, on either side of the termination of the DM. These were also within 500 microns of the termination of DM centrally and between termination of DM and the trabecular meshwork peripherally. In each cluster there were between 2-8 fenestrations of varying sizes 5-60 microns with a mean of 20.3 microns (Figure 4.5).
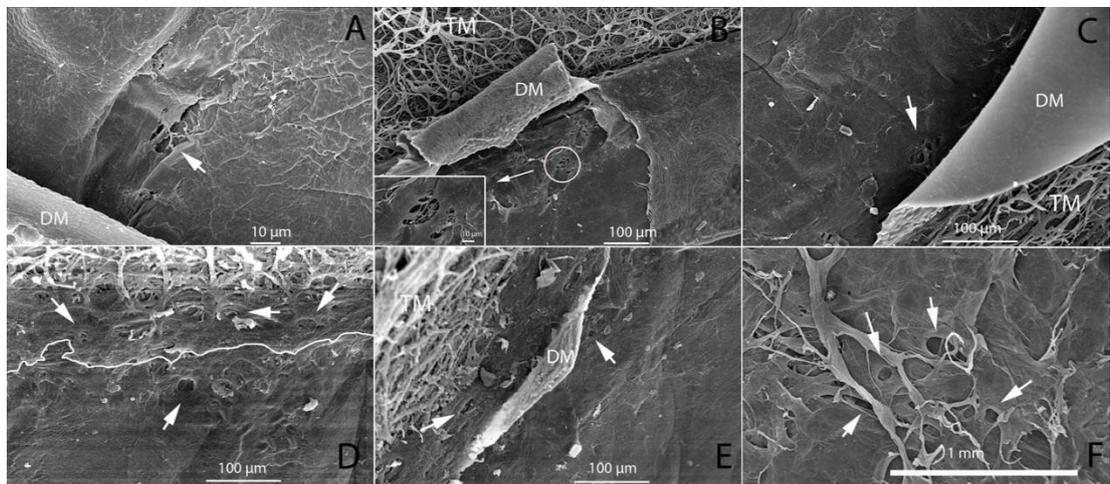
Figure 4.5 Scanning electron photomicrographs. A. The Descemets membrane (DM) has been excised. A cluster of holes (arrow) are visible in the periphery of the pre-Descemets layer (Dua's layer [PDL]). B. The DM at the starting point of a type-2 big bubble has been reflected back on to the trabecular meshwork (TM). A cluster of tiny fenestrations in PDL are seen (white circle). At a higher magnification of this cluster, beams of TM can be seen associated with this area. C. In another sample, the DM at the start of a type-2BB is folded over the TM. A cluster of small fenestrations (white arrow) is seen in the overlying PDL. D. Control sample without injection of air. The DM was removed from the cornea along the white line. Small holes are seen on either side (PDL centrally and TM peripherally) (white arrows) among the origins of the beams of the TM. Air escaping from the peripheral fenestrations would escape in to the anterior chamber during deep anterior lamellar keratoplasty. E. Another control sample without injection of air. Small fenestrations are seen (white arrows) on either side of the DM. F. The central corneal stroma showing multiple holes/spaces (white arrows) from which air escaped to create a type-1BB. The posterior wall of the BB has been removed. (representative photo of approximately 10 samples)

Multiple spaces were seen centrally in the bed (posterior stroma) of type-1BB (Figure 4.5). These were different from the

fenestrations found at the periphery of type-2BB as they were larger, irregular in shape and centrally located.

4.3.4 Light Microscopy

On light microscopy of the samples where air injection was ceased as soon as a complete circumferential band was formed, the doughnut shaped swelling of the circular band was seen to be made up of numerous intrastromal bubbles. The stroma anterior and posterior to the collection of bubbles was compact and devoid of air (Figure 4.3). In the three samples where air injection was ceased as soon as air pockets started to appear in the centre of the cornea, histology showed that the air pockets were located anterior to PDL and were of varying sizes. Some showed evidence of the coalescence of two or more smaller air pockets (Figure 4.4B).

4.4 Discussion

Lamellar corneal surgery has completely changed our approach to corneal transplantation for stromal and endothelial pathology. Most in-vivo and in-vitro (ex-vivo) studies on DALK have centered around the type of BB formed and outcomes of the procedure [63]. Though big bubbles with a 'white margin'; those with a 'clear margin' and 'double bubbles' were well described by Anwar [64] the explanation offered for these appearances was

inaccurate. Anwar described the 'white margin' bubble as a cleavage between stroma and DM and the 'clear margin' and 'double bubbles' as a split between the banded and non-banded zones of the DM. He described BB DALK as a "Descemets baring technique". Later Dua et al 2013 demonstrated that the 'white margin' BB (type-1BB) was due to a cleavage between deep stoma and the PDL; the 'clear margin' BB (type-2BB) was due to a cleavage between PDL and DM and the 'double bubbles' (mixed BB) was due to both types occurring simultaneously. There was never a split between the banded and non-banded zones of DM and as the majority were type-1BB, DALK is not as a rule a 'Descemets baring' technique. In this study, I examined the movement of air in the corneal stroma leading to the formation of a BB and could ascertain that this happens in a fairly consistent manner, providing insight on the structure of the cornea, which is most likely to influence the movement of air. Initial movement of air injected in the central area of the cornea is in the coronal plane corresponding to the predominantly orthogonal (at right angles) arrangement of collagen fibres in the mid and posterior cornea and the lack of a systematic preferred lamellar orientation in the anterior third, where the collagen fibres are largely isotropic (similar in all directions) [65, 66]. The fine 'cracked glass' movement of air in the anterior stroma relates to the compactness of the stroma and is

reminiscent of the needle-like crystalline or Christmas tree pattern formed by microbial colonies in infectious crystalline keratopathy [67]. The anterior 100-120 microns of the cornea has tightly interwoven lamellae which swell less than the posterior two thirds of the stroma [68].

The circumferential movement of air at the periphery was consistent regardless of the initial passage of air. This is a novel and interesting observation that seems to correlate with the peripheral circumferential annulus of collagen and the transition from orthogonal to tangential orientation of fibres as they align with the circumferential annulus [65, 69, 70].

Additional lamellae have also been shown to traverse the peripheral cornea, especially in the posterior region of the cornea [71] conferring greater compactness to this region. Besides, collagen, the presence of a definitive network of elastin fibres in the cornea has been known for some time [72, 73]. Recently, Lewis et al. demonstrated the existence of an annulus of an elastic fibre system in the cornea-scleral limbus, which extends into the posterior cornea as a thin layer, maximally concentrated in the PDL [74]. The circumferential annulus of collagen and elastin fibres, and the compact and the interwoven nature of the collagen lamellae at the periphery could all contribute to the circumferential migration of air and the

relatively limited anterior posterior 'inflation' of this region. Once the periphery of the cornea is filled with air, further injection would force air to move centripetally, and as the posterior collagen fibres are orthogonal and less compact, it would also enable the antero-posterior swelling (with air) of the tissue, observed in the experiments. The relative increased compactness or resistance to expansion, of the stroma at the junction of the peripheral band and the central swollen zone is interesting and requires explanation. This could represent the transition from the orthogonal arrangement of collagen centrally to the tangential arrangement peripherally, as described above [69-71]. As air accumulates in the central cornea it forces its way to the cleavage plane between deep stroma and PDL [4, 8, 28, 75] by separating the deep interwoven lamellae [69] and lifting the PDL together with DM as a type-1BB. It has been shown that the force required to separate the stromal tissue is less in the centre than at the periphery of the cornea [76], which corresponds to the compact stroma at the periphery. This aspect of the architecture of the stroma influences the maximum diameter of a type-1BB, which was shown in this study to extend to the inner circumference of the peripheral band created by the circumferential movement of air. As the type-1BB never occurred in mid stroma or indeed in any part of the stroma other than between the deep stroma and the PDL, it would strongly

suggest that the architecture of PDL is different from the rest of the stroma. The interweave as described by Kokott probably ceases just anterior to PDL to create the plane at which PDL can separate from the deep stroma [69].

This plane of cleavage is also exploited by invading fungi [75], and can also be manifest as a cause or effect of chronic corneal edema [77]. As mentioned above, the accepted architecture of the corneal stroma is described as a closely and tightly interwoven pattern of collagen in the anterior 100-120 microns and a greater spacing of the orthogonally arranged lamellae posteriorly [65, 66, 68]. Dua et al proposed a subtle modification to this description in that the most posterior lamellae in PDL again become tightly packed and are thinner [4]. They reported 5 to 8 lamellae in PDL compared to 3 to 5 lamellae in the corresponding width of stroma immediately overlying the PDL, in an uninflated eye. No air-spaces were noted in PDL indicating that it is impervious to air as has been previously reported [4, 78]. Therefore, as air accumulates under pressure between PDL and the deep stroma, it forces the PDL to separate as a 'bubble'. How then does air traverse PDL to create a type-2BB, wherein air finds the plane between PDL and DM? Data obtained in this study suggests that the clusters of fenestrations present in the periphery of PDL are most likely to provide the passage through which air passes posterior to PDL to lift DM as a type-2BB. This

is consistent with the observation that most if not all type-2BB commence at the periphery. However, in mixed bubbles, a different mechanism can operate. As the type-1BB expands to its maximum diameter, air can leak through the stretched fibres of PDL at the periphery of the bubble to find the plane between PDL and DM. This mechanism was the exception.

The compact fibres of PDL have been shown to separate and fan out as the collagen core of the trabecular meshwork [5] at the periphery of PDL. Separation of collagen lamellae can cause spaces to appear and present as fenestrations reported herein. The physiological role of these fenestrations is unclear but in BB DALK they play an important role in determining the formation of a type-2BB. Moreover, the appearance of tiny bubbles of air in the anterior chamber during BB DALK is a common observation. This is largely attributed to the escape of air from the trabecular meshwork into the anterior chamber [8] . In this study, it was noted that some fenestrations are located distal to the attachment of the DM, between the termination of DM and the origin of the trabecular meshwork and at times between the trabecular meshwork and sclera. Air escaping from these holes would find access to the anterior chamber and is most likely the route through which air bubbles appear in the anterior chamber. Such holes or fenestrations between the termination of DM and

trabecular meshwork were noted in all samples where peripheral leaking points were marked and studied by SEM.

This study shows that air moves in a consistent pattern in the corneal stroma, which corresponds to the known architecture and disposition of stromal collagen in the central and peripheral stroma. Spaces between interwoven lamellae appear to permit and direct intrastromal movement of air to the plane anterior to PDL and create a type-1BB. The demonstration of multiple clusters of fenestrations in the periphery of the PDL, adjacent to the trabecular meshwork, is a novel addition to the microanatomy of the peripheral cornea and provides a valid explanation for the egress of air through PDL, to create a type-2BB, and into the anterior chamber during DALK. Despite the initial controversy [16, 61] the lack of air-spaces in PDL and its impervious (to air) nature; the concentration of elastin fibres in PDL [74] and the fact that a type-1BB cannot be obtained following ablation of PDL by phototherapeutic keratectomy [79], and its recent demonstration in-vivo by ultrahigh resolution OCT [80], all point to its unique nature.

CHAPTER 5

OPTICAL COHERENCE TOMOGRAPHY CHARACTERISTICS OF DIFFERENT TYPES OF BIG BUBBLES SEEN IN DEEP ANTERIOR LAMELLAR KERATOPLASTY BY THE BIG BUBBLE TECHNIQUE.

5.1 Introduction

Deep anterior lamellar keratoplasty (DALK) is considered the gold standard procedure for corneal transplantation where best corrected vision is affected by scars, dystrophy or ectasia involving corneal stroma. The most popular technique is Big-Bubble(BB) technique [28] wherein air is injected in the corneal stroma to separate either Descemet's membrane(DM) or DM together with a layer of deep corneal stroma termed pre-Descemet's layer(Dua's layer–DL). This allows replacement of affected stroma with healthy stroma from a cadaver donor.

Injection of air into human corneal stroma produces three different types of BB [4]: 1. Type-1, where air cleaves DL from posterior stroma; BB starts at the centre and spreads centrifugally to a maximum diameter of 8.5 mm. 2. Type-2, where air cleaves DM from stroma. This type starts from corneal periphery and spreads across the posterior surface of the cornea reaching a maximum diameter of 10-10.5mm. 3. Mixed-BB, where both type-1 and type-2 appear together. Usually type-1 is

complete and type-2 is partial. Rarely both are complete with type-2 enclosing type-1 within [4, 62].

Knowing which type has formed intra-operatively is very important as type-2 and type-2 component of a mixed-BB are vulnerable to tearing or bursting. This can be avoided by taking necessary precautions. Clinical clues such as the point of origin and BB size as described above and the 'rough' appearance of the wall of type-1 seen after excising the stroma compared to very smooth appearance of type-2 [81] help distinguish type-1 from type-2. Recognising mixed-BB intra-operatively is difficult. Anecdotal presentations at meetings of images from intraoperative optical coherence tomography (OCT) have indicated that this might be the definitive way of recognising the different types of BB.

OCT offers non-contact, real time, cross-sectional images, which were hitherto impossible to acquire [46, 47, 50]. Since its introduction in 1994 by Izatt et al, anterior segment OCT has become an essential tool in clinical diagnosis and follow up of many ocular pathologies [48, 82, 83]. OCT of anterior segment provides image resolution of 1 to 15 μm in both axial and lateral directions. This resolution is finer than conventional imaging modalities such as ultrasound, magnetic resonance imaging (MRI), or computed tomography (CT) [50, 84]. Furthermore, image acquisition does not require topical anaesthesia or a water

bath [85]. Two types of OCT are in common use, Time-domain (TD-OCT) and Fourier-domain (FD-OCT). TD-OCT (Visante) has a resolution of 18μm and scan speed of 2048 A-scans per second. FD-OCT (Spectralis and Topcon), which can provide more detailed cross-sectional images of the biological structures, has an axial resolution of 5μm and at least ten times faster scan speed. Thus, FD-OCT is faster than TD-OCT, reduces artefacts and improves resolution. In contrast, the TD-OCT penetrates deeper in the sclera, cornea and the iris than the FD-OCT due to its longer wavelength of 1310nm compared to 840nm of FD-OCT [82, 86].

In this study I undertook OCT examination and analysis of different types of BB created in eye bank donor eyes and ascertained characteristics which will enhance our understanding of the BB anatomy [87] and inform and help surgeons to interpret real-time OCT images during DALK and other posterior segment surgery.

5.2 Materials and methods

Thirty human sclero-corneal discs maintained in organ culture in Eagle's minimum essential medium with 2% foetal bovine serum for four to eight weeks post-mortem were used for scanning with Spectralis and Topcon OCT systems. Donor details (age, sex and cause of death) are given in Table 5.1. Donor tissue was obtained from National Health Service Blood and Tissue (NHSBT) eyebank, Manchester, UK.

Table 5.1 Donor information for sclero-corneal samples included in the experiments.

Sample Number	Sex	Age	Cause of death
E875	F	56	Renal cancer
M17915B	F	93	Pneumonia
E18037A	unknown	unknown	unknown
E917	F	69	Intracranial heamorrhage
E948	M	79	Pneumonia
E1208	M	66	Unknown (other)
E1046	unknown	unknown	unknown
E1132	M	76	Cancer
E1170	F	80	Unknown (other)
E877	F	92	COPD
E1072	M	84	Pancreatitis

E1074	F	93	Dementia
E1881	M	60	Unknown (other)
E1911	F	83	Pneumonia
E1914	F	67	Unknown (other)
E1950	M	82	Lung Cancer
E1985	F	74	Unknown (other)
E1959	unknown	unknown	unknown
E1879	M	78	Unknown (other)
E1878	M	78	Unknown (other)
E1856	M	79	Chronic pulmonary disease
E1839	M	65	Pneumonia
E1910	F	83	Pneumonia
E1909	M	89	Pneumonia
E1917	F	75	Respiratory failure
E1954	F	78	Encephalopathy
E2030	M	76	Unknown (other)
E2054	M	69	Pneumonia
E2051	F	82	Cerebro vascular accident
E1854	F	78	Respiratory failure

5.2.1 Air injection

The sclero-corneal discs were removed from storage medium and placed in a petri-dish, endothelium-side up, and covered with balanced salt solution. Under an operating microscope, a 30-gauge needle, bevel-up, attached to a 5-ml syringe was passed from the scleral rim into the corneal stroma and advanced to the centre of the disc. The needle was passed close to endothelial surface without perforating it. Air was injected with force to overcome the tissue resistance, until a big bubble was formed. The BB type was ascertained and the samples fixed in 10% formalin.

Two samples of each type of BB were scanned without fixation and compared to images obtained from formalin fixed samples.

5.2.2 Optical Coherence Tomography

Twelve samples (3 type-1, 3 type-2, 3 mixed and 3 type-1 from which DM had been partially peeled) were examined with Topcon OCT (3D-OCT-2000) system (Topcon Corporation, Tokyo, Japan). Eighteen samples (5 type-1, 3 type-2, 6 mixed and 4 type-1 from which DM had been partially peeled) were examined with Spectralis OCT (Spectralis, Heidelberg, Germany).

A special clamp with a long flexible arm that could be affixed to the OCT table or head-rest frame at one end and a ball-and-socket type joint allowing movement in any direction attached to an artificial anterior chamber (AAC) holder at the other end was used. The sclero-corneal disc with the posterior surface out (surface with BB) was mounted on AAC (Katena, Denville, NJ, USA), the chamber was filled with BSS and AAC tubing was closed. AAC carrying the sample was mounted in the holder and positioned such that BB was perpendicular to the objective of OCT equipment. Using 'Cornea' mode of OCT machine, BB was scanned to get average 10 scans per sample. Representative scans were selected and the thickness of BB wall and its components were measured using equipment software.

Sixteen additional samples (5 type-1, 4 type-2, 3 mixed and 4 type-1 from which DM was partially peeled) from University of British Columbia, Vancouver, were examined with the Visante OCT system (Carl Zeiss Meditec AG, Jena, Germany). This provided wide angle images of BB. These samples were stored in Optisol (Chiron Ophthalmics, Irvine, California) at 4^0C. OCT imaging was performed soon after air inflation in these samples. As with previous examinations, samples were scanned with BB facing the OCT system. Images were captured using "Enhanced Anterior Segment Single" mode and exported to image-J for evaluation. Mean and standard deviation of measurements from

all scans were calculated, for each instrument used. Donor details are given in Table 5.2.

Table 5.2 Donor information of the sclero-corneal samples scanned by Visante OCT.

Sample Number	Sex	Age	Cause of Death
0071OD	M	51	Lung Cancer
0189OD	M	53	Cardiac arrest
0189OS	M	53	Cardiac arrest
0294	F	42	CVA
0030OD	M	63	Squamous cell carcinoma
0059OS	F	71	Peritoneal Carcinoma
0260	M	63	Renal carcinoma
0233OS	F	63	Lung carcinoma
0233OD	F	63	Lung carcinoma
0059OD	F	71	Peritoneal carcinoma
0214	M	55	Pancreatic carcinoma
0352	F	65	Cancer
0071OD	M	51	Lung Cancer
0189OD	M	53	Cardiac arrest
0189OS	M	53	Cardiac arrest
0294	F	42	CVA

5.3 Results

For NHSBT eyes, mean donor age was 70 years. There were 13 males and 14 females. Information was not available for three donor eyes. Cause of death varied and in some it was unknown and coded as 'other'. Mean donor age was 57 years for Vancouver donor eyes. There were 9 males and 7 females.

In type-1, both Topcon and Spectralis OCTs of the posterior wall revealed parallel, double-contour, hyper-reflective curved line with hypo-reflective space in between (Figure5.1 A & 5.2 A). In type-2, OCT also revealed a parallel, double-contour curved hyper-reflective line with a dark space in between (Figure 5.1B & 5.2B). The anterior line was narrower than that seen with a type-1(Figure 5.1B & 5.2B). In the mixed-BB, OCT showed two separate

curvilinear images (Figure 5.1C & 5.2C) one with double-contour and the other as single hyper-reflective image.
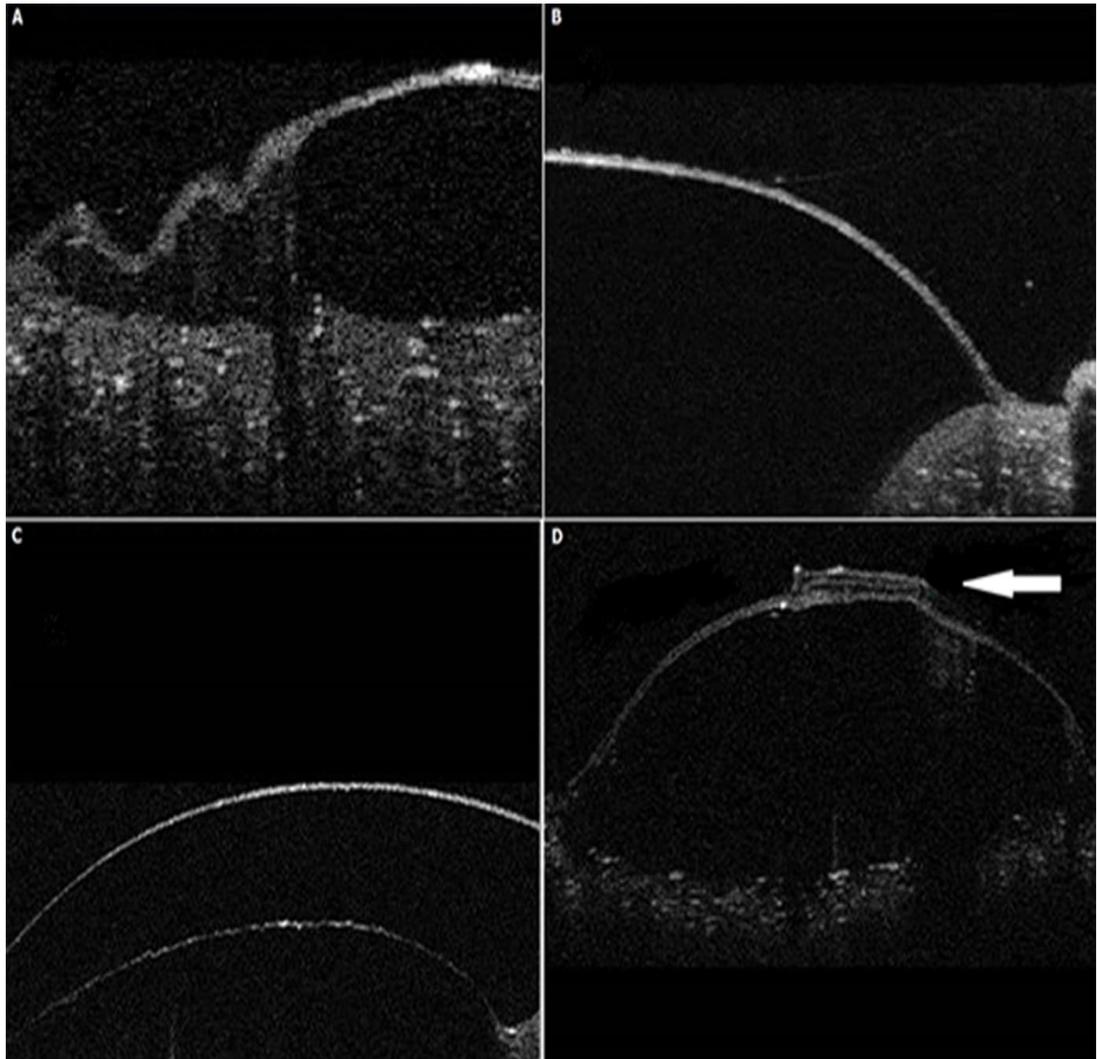
Figure 5.1 Topcon OCT: (A) Type-1 Big bubble (BB) showing two curvilinear lines. The anterior line represent Dua's layer (DL) and banded zone of Descemet's membrane (DM). (B) Type- 2 BB showing two curvilinear lines that represent banded and non-banded zones of DM. (C) Mixed BB where the anterior line represents DL and the posterior line represents DM. (D) Type-1 BB from which the DM was partially peeled off. The peeled DM is folded on itself (arrow). The OCT image to the right of the peeled DM is a single line and that to the left has a double-contour as seen in the posterior wall of a type-1 BB. (representative photo of approximately 15 samples)

When DM was peeled-off type-1, OCT showed only single hyper-reflective curved line corresponding to the anterior line of the double-contour line described above (Figure 5.1D & 5.2D). On the other hand, Visante OCT of the posterior wall of type-1 and type-2 BB showed a single hyper-reflective curved line rather

than the double-contour line. However, it captured the entire bubble diameter, whereas with FD-OCT only part of BB could be imaged at any one time (Figure 5.3).
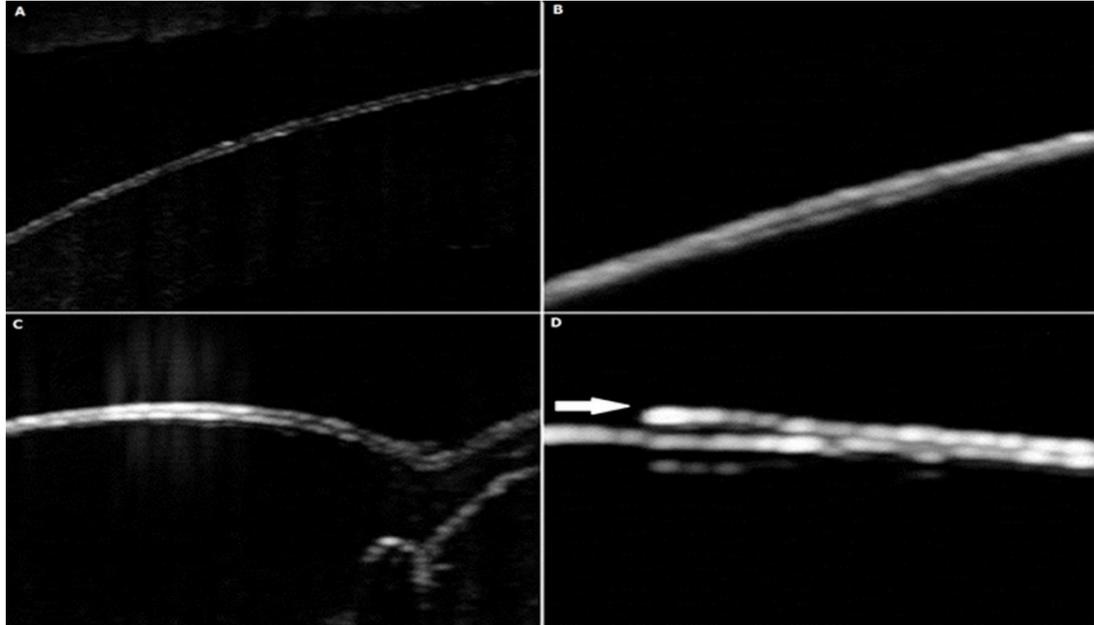
Figure 5.2 Spectralis OCT: (A) Type-1 Big bubble (BB) two curvilinear lines exist. The anterior line represents Dua's layer (DL) and banded zone of Descemet's membrane (DM). (B) Type-2 BB showing two curvilinear lines that represent banded and non-banded zones of DM. (C) Mixed BB where the anterior line represents DL and the posterior line represents DM. (D) Type-1 BB with DM from which the DM was partially peeled off. The peeled DM is indicated by the arrow. (representative photo of approximately 15 samples)

Topcon OCT measurements are shown in Table 5.3. The mean thickness of DM was 41.5+/-2.7µm and that of DL was 24.3+/-2.8µm. However, the mean of DL+DM was 49.6+/-5.3µm, which was not the sum of DL and DM separately. Also, results showed that the mean of DL+DM banded zone (DMB) which represents the anterior line of the posterior wall of type-1, was 18.1+/-1.6µm, whereas the anterior line of type-2 measured 16.7+/-

1.59µm, which is slightly less than that of DL+DMB. Furthermore, the mean thickness of DL in mixed-BB and peeled part of type-1 was 26.0+/-2.8µm and 22.6+/-1.6µm respectively.
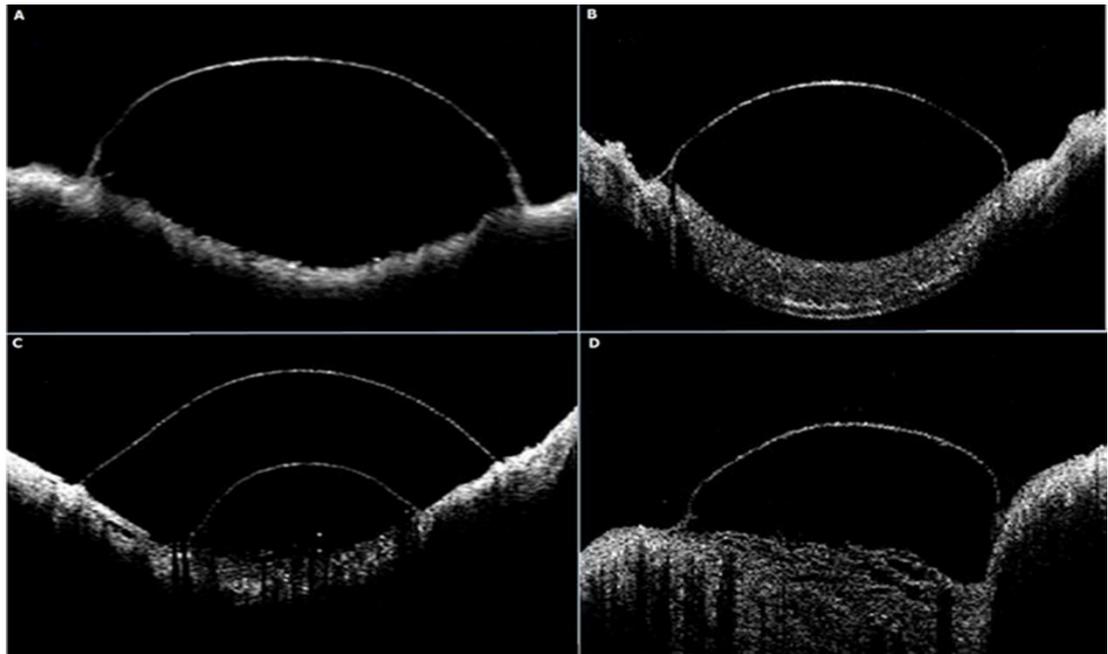
Figure 5.3 Visante OCT: (A) Type-1 Big bubble (BB) where the single curvilinear line demarcated the entire extent of the BB. (B) Type-2 BB where the image is similar to that seen with a type-1 BB. (C) Mixed BB where the OCT scan was performed at the location of the two bubbles. The upper (posterior) line represents Descemets membrane (DM) and the lower (anterior) line represents Dua's layer. The DM line does not demonstrate a 'double-contour' as is seen with the Topcon and Spectralis machines. (D) A type-1 BB from which DM was peeled off. The OCT image is like the DL image of a mixed BB. (representative photo of approximately 15 samples)

Spectralis OCT measurements are shown in Table 5.3. The mean thickness of DM was 25.8+/-5.8µm and that of DL was 19.1+/-3.3µm. However, the mean of DL+DM was 36.7+/-4.6µm, which is not the sum of DL and DM separately. Also, results showed that the mean of DL+DMB which represents the anterior line of a

type-1 was 14.1+/-2.4µm, whereas the anterior line of a type-2 measured 10.4+/-0.9µm, which is less than that of DL+DMB. Mean thickness of DL in mixed-BB and the peeled part of type-1 was 18.7+/-2.6µm and 19.6+/-4.1µm respectively.

Visante OCT measurements are shown in Table 5.3. All values were greater than those with the other two devices. Mean thickness of DM was 53.1+/-18.6µm and that of DL was 51.0+/-15.6µm. The mean of DL+DM was 72.6+/-15.5µm, which is not the sum of DL and DM separately. The posterior wall of type-1 and type-2 BB presented as a single curvilinear hyper-reflective image unlike the corresponding images obtained with the other two devices. Mean thickness of DL in mixed-BB and the peeled part of type-1 was 56.6+/-22.2µm and 46.7+/-3.9µm respectively.

No difference was noted in the samples measured 'fresh' and the same samples after fixation in formalin for up to 48 hours.

Table 5.3 Topcon, Visante and Spectralis OCT measurements of the posterior wall of the big bubbles.

Topcon	Sample Number	Type of Bubble	DL (microns)	DM (microns)	DL+DM (microns)	DL+DMB (microns)	DMB (microns)
	E875	T1BB			54	16	
	M17915B	T1BB			48	18.33	
	E18037A	T1BB			53	20	
	E917	T2BB		40.3			16
	E948	T2BB		39.33			19
	E1208	T2BB		38.66			15.33
	E1046	MB	24	41			
	E1132	MB	30	43			
	E1170	MB	24	47			
	E877	PB	22		40		
	E1072	PB	25		47		
	E1074	PB	21		56		
Spectralis	E1881	T1BB			34.3	13.3	
	E1911	T1BB			34	14	
	E1914	T1BB			36.3	16.6	
	E1950	T1BB			28	10	
	E1985	T1BB			38.3	16.6	
	E1959	T2BB		29			10.33
	E1879	T2BB		23.66			9.33
	E1878	T2BB		39.6			11.66
	E1856	MB	17	22			
	E1839	MB	22	24			
	E1910	MB	16	21			
	E1909	MB	15.7	25.5			
	E1917	MB	21	19			
	E1954	MB	21	29.3			
	E2030	PB	20.6				
	E2054	PB	16		39		
	E2051	PB	26		45		
	E1854	PB	16		39		
Visante	0030OD	T1BB			98		
	0071OD	T1BB			80		
	0189OD	T1BB			69		
	0189OS	T1BB			64		
	294	T1BB			52		
	0095OS	T2BB		28			
	0233OD	T2BB		33			
	0233OS	T2BB		75			

	260	T2BB		35			
	0095OD	MB	32	65			
	214	MB	86	69			
	253	MB	52	67			
	0071OD	PB	46				
	00189OD	PB	46				
	00189OS	PB	53				
	294	PB	42				

DM: Descemet's membrane. DL: Dua's layer. DMB: Descemet's membrane (Banded zone). MB: Mixed Bubble. PB: Peeled Bubble. T1BB: Type 1 Big Bubble. T2BB: Type 2 Big Bubble. Each figure is the mean of 3 measurements taken equidistant along length of each sample.

5.4 Discussion

I was able to reproduce the different BB types as reported by Dua et al 2013 [4]. OCT images could be obtained for all types of bubbles but the scan had to be performed with the posterior surface of BB facing the objective. This was due to the multitude of tiny bubbles or pockets of air in the corneal stroma which created many artefacts and prevented acquisition of good images of the posterior wall of BB. Moreover, with FD-OCT the depth range of OCT system did not extend as far as the posterior wall of BB. Hence for consistency, with TD-OCT also, scanning was performed with the posterior wall facing the objective lens. In order to understand the description and measurements it is

therefore important to bear in mind that the convex surface of the OCT image of BB represents the posterior surface, and the concave surface of the image represents the anterior surface.

The characteristics of the images of the posterior wall of different BB examined were very similar for both Topcon and Spectralis equipment but resolution was slightly better with Spectralis than with Topcon. The posterior wall of type-1, which is made of DL anteriorly and DM posteriorly and of type-2 made of DM alone were both seen as parallel, double-contour, curvilinear hyper-reflective images. The two hyper-reflective linear images were separated with narrow hypo-reflective dark line. In type-2 the anterior line was thinner than that seen in type-1. By direct observation it was difficult to discern which anatomical component contributed to which component of the OCT image.

On comparing the images of type-1 and type-2 BB it was evident that DM independently produced a parallel, double-contour, hyper-reflective image with the two lines separated by dark space. By inference the two lines should therefore represent the banded zone (anterior line) and non-banded zone (with endothelium-posterior line) of DM. This observation has been reported with the use of ultrahigh-resolution OCT imaging of normal corneas and corneas with Fuch's endothelial dystrophy

[88-90] and is seen in OCT images reported by others but has not been specifically commented on [91]. In OCT image of type-1 BB the anterior line would correspond to the banded zone and DL. Though this was thicker than that of the anterior line seen in type-2, the difference was only 2(Spectralis) to 4(Topcon) microns. The total thickness of the posterior wall of a type-1 BB was 36(Spectralis) to 49(Topcon) microns whereas that of a type-2 was 25(Spectralis) to 41(Topcon) microns. This would be expected as the posterior wall of type-1 BB is made of DL+DM. Interestingly however, the thickness of DL alone as measured after peeling-off DM from type-1 or from mixed-BB was 19(Spectralis) to 24(Topcon) microns producing an anomaly in that the sum of DL and DM measured individually did not add up to the thickness of the posterior wall of a type-1 BB, which is formed by these very same layers together. This could be due to inaccuracy in the measuring tool provided in the software of the equipment, especially in the range of thickness being measured or more likely to an artificial widening of the hyper-reflective images due to light backscatter [50]. This error could also be inherent in the automatic adjustment of the intensity scale applied by different equipment. Such artefactual widening would affect each layer individually thus amplifying the thickness measurement of each, making the sum of the two greater than the measure of the two layers closely applied to each other.

Dua et al 2013 reported that DL measures around 10.1+/-3.6µm on transmission electron microscopy [4] The difference of this measurement from our OCT measurements is probably due to the fact that OCT images display biological tissue structure in a way different from the actual histological thickness. Moreover, measurements from histology sections do not accurately reflect the true thickness as tissue preparation for microscopic examination is associated with tissue dehydration. Fujimoto et al. [50] state that "In OCT, image contrast occurs from intrinsic differences in tissue optical properties. Thus, care must be taken when interpreting OCT images, since they are not analogous to conventional histology". Furthermore, refraction at several boundaries, high index of the cornea and the added element of back reflection and scattering of light beam from corneal tissue would render OCT images thicker and different from histological images [49, 50]

The basis of mixed bubbles was first explained by Dua et al who demonstrated that these were due to type-1 and type-2 BB occurring simultaneously with type-2 usually being partial and type-1 complete though both can be complete [4]. Mixed-BB had been observed by surgeons prior to the report by Dua et al but were attributed to a split in banded and non-banded zones of DM. OCT images of mixed-BB confirmed that the type-2 component was made of the full thickness of DM with parallel,

double-contour line and an additional single hyper-reflective image of DL separated from DM by dark space (intervening air). When DM was partially peeled off type-1 BB, OCT image of the remaining underlying tissue (DL) revealed single hyper-reflective line similar to that of type-1 component of mixed-BB. Adjacent unpeeled wall retained its double-contour configuration indicating that this was a feature of DM alone.

Visante OCT produced wide field images of the bubbles but the resolution of images was poor compared to the other two. In Visante images, DM appeared as a single hyper-reflective line. The measurement of thickness of the wall of type-1 with Visante OCT was 72.6+/-15.5µm, which is much thicker than that obtained with other devices. Similarly, the thickness of DM and DL with Visante OCT was 53.1+/-18.6µm and 51.0+/-15.6µm respectively, which were also much thicker than the measurements obtained from the other two devices. The low image resolution and higher backscatter intensity of light with Visante can explain the difference.

This study has helped to elucidate important OCT characteristics of the posterior layers of the cornea, which have implications for corneal surgery, especially with the advent of intra-operative OCT. Intra-operative OCT is proving to be a useful tool in aiding surgeons in a variety of procedures [92, 93]. The study has also provided evidence to support clinical observations made in ex-

vivo experiments on human eyes in particular with regard to the different types of bubbles and the nature of mixed-BB. With the ongoing development of ultrahigh-resolution OCT and its introduction in clinical practice, direct observation both in-vivo and ex-vivo, of anatomical details of the cornea will be possible.

CHAPTER 6

ENDOTHELIAL CELL LOSS FOLLOWING TISSUE HARVESTING BY PNEUMO-DISSECTION FOR PRE-DESCEMETS ENDOTHELIAL KERATOPLASTY (PDEK) AND DESCEMETS MEMBRANE ENDOTHELIAL KERATOPLASLTY (DMEK): AN EX VIVO STUDY.

6.1 Introduction

Injection of air in the stroma to produce a big bubble is the most popular technique for deep anterior lamellar keratoplasty (DALK). Until recently it was believed that air stripped off the Descemets membrane (DM) from the posterior stroma allowing removal of the diseased stroma and replacement by healthy stroma from eye bank eyes. In some instances 'explosive bubbles' and 'funny or double' bubbles were described wherein in one sector, a bubble within a bubble was noted. This was attributed to a split between the banded and non-banded zones of the DM.[94] Several authors have also communicated, at international meetings, the occurrence of bubbles that burst during surgery and the operation had to be converted to a penetrating keratoplasty. This is also our own personal experience.

Recently Dua et al provided explanations for several unexplained features of the big bubble DALK operation and related it to hitherto unknown aspects of the behaviour of the deep posterior human corneal stroma.[4] Air injection was performed on human sclera-corneal discs and it was noted to spread from the site of injection, circumferentially and posteriorly to fill the corneal stroma and eventually result on the formation of a Big Bubble (BB).[62]

Three types of BB were noted. Type-1 BB which is a well circumscribed, dome-shape, central elevation. The bubble size ranged from 6.5 to ≤9 mm in diameter. This bubble started at the central part of the cornea then spread circumferentially to the periphery. Type-2 BB, which has a thin wall and measures a maximum 10.5 mm in diameter. It always started as a small bubble from the periphery and then expands centrally to form a larger big bubble. A mixed type of big bubble was also noted. This consists of a Type-1 and a smaller Type-2 Bubble which exists at the periphery of the Type-1or it may exist as a Type-1 BB in the centre covered with a larger Type-2 Bubble which extends to the periphery.[62]

They further characterised the layer [5] and also demonstrated that the DM was not essential for the formation of a Type-1 BB as the DM could be peeled off the Type-1 BB without deflating it

and also that a Type-1 BB could be consistently created after first removing the DM.[62]

Pneumo-dissection of the DM from donor corneas (as with Type-2 BB) to harvest tissue for Descemet's membrane endothelial keratoplasty (DMEK) has been reported.[95-99] The composite of DL and DM with endothelium harvested from Type-1 BB has been used in one type of endothelial keratoplasty termed Pre-Descemet's endothelial keratoplasty (PDEK).[43] Prior to the description of the different cleavage planes in the different types of BB surgeons had injected air in donor corneas to obtain tissue for DMEK and assumed that they were harvesting DM and endothelium.[43, 95-97] It is suggested that PDEK might become as popular if not more, than DMEK in the years to come. In this experiment, I studied ex-vivo the endothelial cell counts in PDEK and DEMK tissue obtained from eye bank donor corneas to ascertain whether there were any differences related to the specific method of pneumo-dissection used to harvest tissue for transplantation.

6.2 Materials and methods

Twenty sclero-corneal discs from human eye bank donor eyes were studied. Samples were kept in organ culture in Eagle's minimum essential medium with 2% foetal bovine serum for four to eight weeks post-mortem. Five consecutive samples with Type-1 BB (figure 6.1a) and five consecutive samples with Type-2 BB (figure 6.1b) were used, each with its own control sample. Tissue for PDEK and DMEK respectively were obtained from these samples. In order to obtain the 10 test samples for the study a total of 32 samples were injected.
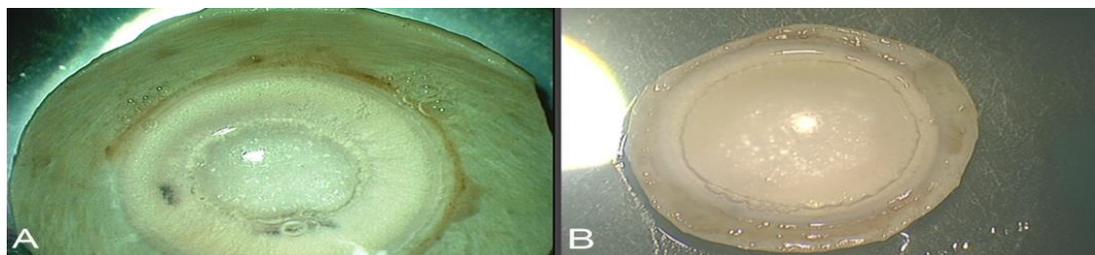
Figure 6.1 Examples of Type-1 (a) and Type-2 (b) big bubbles from which tissue for PDEK and DMEK respectively were obtained. Cataract incisions are visible in the donor sclero-disc in (a).

As there was many more Type-1 BB obtained, we continued to inject until we got the requisite number of type 2 big bubbles as well. Details of the donor tissue used in the study are given in table 6.1.

Table 6. 1 Donor details for the sclero-corneal discs used in the experiments.

Number	Sex	Age*	Type of BB	Cause of Death
1	M	89	Type-1	Pneumonia
2	F	83	Type-1	Pneumonia
3	F	83	Type-1	Pneumonia
4	F	45	Type-1	Multi-organ failure
5	F	45	Type-1	Multi-organ failure
6	F	67	Control	Other
7	M	78	Control	Not Reported
8	M	78	Control	Not Reported
9	M	60	Control	Not Reported
10	M	60	Control	Not Reported
11	F	71	Type-2	Intracranial–Type unclassified (CVA)
12	F	71	Type-2	Intracranial-Type unclassified (CVA)
13	M	66	Type-2	Respiratory
14	M	66	Type-2	Respiratory
15	M	78	Type-2	Chronic pulmonary disease
16	F	66	Control	Respiratory failure
17	M	84	Control	Septicaemia
18	M	79	Control	Chronic pulmonary disease
19	M	79	Control	Chronic pulmonary disease
20	M	65	Control	Pneumonia

BB = Big bubble. *Mean age of Type-1= 69 years, Type-1 control=68.6 years, Type-2= 70.4 years, Type-2 control= 74.6 years.

6.2.1 Pre-injection endothelial cell counts

Endothelial cell counting was done using a phase contrast microscope (Nikon, Kingston upon themes, Surry, UK.) with an eyepiece reticle with 10x10 grids of 1 mm indexed squares. 100x1 mm squares in the 10x10 grid are indexed 1-10 along top and A-J downs the side (Pyser-SGI Limited, Kent, UK). A micrometer slide (Thermo Scientific, Braunschweig, Germany) was placed on the stage to calibrate the reticle (grid). The length and width of 2 small squares at the magnification used (x10 objective and x10 eye piece) measured 0.192 mm x 0.192mm. Ten readings of cell counts were taken from different randomly selected areas of the sample corneal endothelium. Each area corresponded to 2x2 squares (0.036864 mm^2). The average of the ten readings was then calculated and converted to area in mm^2 (average/0.0368).

6.2.2 Preparation of PDEK and DMEK tissue

The donor sclero-corneal discs were removed from the storage medium and placed in a petri dish, endothelial side up, and covered with balanced salt solution. Under an operating microscope, a 30 gauge needle, bevel up, attached to a 5 ml syringe was passed from the scleral rim into the corneal stroma and advanced to the centre of the disc to lie close to the

endothelial surface. Air was injected with sufficient force to overcome the tissue resistance, until a big bubble was formed.

The Type of the bubble, Type-1 or Type-2, was noted and the tissue processed for cell counts. A control sample consisted of another sclero-corneal disc treated similarly with regard to placement in a petri dish for the same duration as the test sample, but without injection of air.

6.2.3 Post injection endothelial recounting

Sample corneas with big bubble were deflated by aspirating the air and replaced in Eagle's minimum essential medium, for recounting the endothelial cells.

In the laboratory, the sclera-corneal discs with the deflated bubbles were trephined (6mm) from the posterior surface. Tissue samples thus obtained from a Type-2 BB were of Descemet's membrane and endothelial cells alone and from a Type-1 bubble were of Descemet's membrane, endothelial cells and Dua's layer. The samples were spread on a glass slide and endothelial cells re-counted as described above. Both types of tissue were handled similarly.

6.2.4 Controls

Human donor samples without air injection were used as controls. Control samples were treated in exactly the same

manner as the test samples with the exception of the air injection step. They were subjected to the same environmental and laboratory conditions as the test samples, i.e. they were removed from storage and placed in a petri dish on the operating table beside the sample to be injected, for the same duration, before replacing in tissue culture medium. Endothelial cells were counted at the same time points as the test samples. Results were then analysed and compared with the test samples using the GraphPad Prism 6 software (Graphpad software Inc., La Jolla, USA).

6.3 Results

The average age of the donors was 70 years (range 45-89 years). They were 12 males and 8 females. The cell counts obtained in test samples and controls are given in Table 6.2. Though there was a wide variation in the cell counts of individual samples, there was no statistically significant difference between controls and test samples pre-injection.

With Type-1 BB (PDEK tissue) there was no statistically significant different in the endothelial cell counts pre and post injection. However, there was a significant difference ($P < 0.05$) when we compared DMEK test samples before and after injection. Also, there was a significant difference ($P < 0.05$) between DMEK test samples (post injection) and their controls.

Table 6.2 Cell counts per mm² and statistical significance of test samples and controls before and after injection.

	PDEK			DMEK		
N=5 (each group)	Sample	Control	P Value	Sample	Control	P Value
Pre-bubbling cell count/mm²	996.8 +/- 284.5	1072 +/- 339.0	0.276	1267 +/- 273.7	1393 +/- 315.8	0.241
Post-bubbling cell count/mm²	943.8 +/- 273.9	1014 +/- 282.6	0.253	1096 +/- 178.7	1363 +/- 321.5	0.028* (P<0.05)
Pre-bubbling Vs Post-bubbling P Value	0.0512	0.1686		0.0456* (P<0.05)	0.086	

*Reached statistical significance

The range of change of endothelial cell density (ECD) before and after injection in PDEK sample groups varied from (-9 to +0.2%) [a minus value indicates a loss of endothelial cells and a plus value indicates a gain], with an average of -5.36% +/- 3.8%. On

the other hand, the range of change of the ECD of the DMEK group before and after injection varied from (-0.4 to −20.6), with an average of -12.44% +/- 8.11%.

6.4 Discussion

Improved understanding of the microanatomy of the posterior cornea, in particular the surgical anatomy, [4, 62] has led to the innovation of two surgical procedures, DALK-Triple [14] and PDEK.[43] Though "PDEK" might have been inadvertently performed by others before, they had described this as DMEK [43, 95-98] or DMEK with stromal support (DMEK-S).[100] PDEK in its current established form was proposed by Dua HS and first performed by Agarwal et al.[43] The fact that a Type-1 BB can be created in donors of any age (our unpublished observations) would allow very young tissue with consequent higher endothelial counts to be used for PDEK compared to the conventional stripping technique used to obtain tissue for DMEK wherein it is recognised that the risk of tissue loss is greater in older donors. [101, 102] Moreover the support afforded by DL makes the tissue easier to handle and unroll in the eye compared to DM alone. Agarwal et al [43] also demonstrated good graft attachment with good visual recovery post operatively. Four patients out of five, gained corrected distant visual acuity of 20/30 and one patient gained 20/40. These

results suggested that endothelial cell function was adequate after PDEK [43] though they did not assess endothelial cell counts in their study.

In this experiment I aimed to provide objective evidence of endothelial cell counts by assessing endothelial cell loss that could result from the steps employed in preparation of PDEK graft tissue and compare it with endothelial cell density of DMEK graft tissue obtained by the same technique. The samples I used in were from different age groups and some of them were from eyes that had previous cataract surgery. Some samples were unpaired (two PDEK and two DMEK) with their controls (i.e. the control was not from the same donor, as often only one eye from a given donor was available for study).

However, despite the above limitations I did not find any significant difference between PDEK and DMEK samples and their controls at baseline. On the other hand, a significant difference was noted in the DMEK group before and after bubbling and also between DMEK samples and their controls post bubbling. The same comparison of PDEK tissue with controls and the difference between pre and post bubbling was not significant. This indicates that the steps involved in PDEK tissue preparation result in less endothelial cell loss compared to DMEK tissue preparation by this

technique. Though there was no statistically significant cell loss during PDEK tissue preparation it showed a trend towards cell loss that might be significant with a larger number of samples. However, it can be concluded on the basis of this study that the endothelial cell loss with PDEK tissue preparation is no worse than that with DMEK tissue preparation by the pneumo-dissection method. This coupled with the clinical results from PDEK observed thus far would suggest that PDEK is a viable endothelial transplant procedure.

Moreover, clinical evidence from BB DALK procedures, which employ the same principle as PDEK (when Type-1 BB are obtained) and DMEK (when Type-2 BB are obtained) also suggests that bubbling per se does not lead to significant endothelial cell loss as DALK eyes retain good corneal clarity and show less cell loss compared to eyes after penetrating keratoplasty.[103, 104]

Busin et al demonstrated in an ex-vivo study that the endothelial cell loss after pneumatic dissection for DMEK was 4.44 +/- 4.3% after 7 days of tissue culture medium storage.[96] Another study conducted by Yoerueket al [105]comparing pneumatic and forceps dissection of DM showed that the mean endothelial cell density after pneumatic DMEK graft had declined from 2038+/-212 mm to 1863+/-211 mm.[105] However, this was before

knowledge of Dua's layer was widely known and previous studies are likely to have included both type 1 and type 2 big bubbles as 'DMEK' tissue obtained by pneumo-dissection.

Another method proposed by Parekh M et al [106]employed a standardized submerged hydro-separation of DM to prepare DMEK tissue graft from donor corneas. They found that the endothelial cell loss after preservation was 11.48%.[106] Though the similarity in endothelial cell loss is comparable to this study one has to consider the fact that statistics from in vivo studies are biased in that they did not include DMEK grafts that detached early. Early detachment could be related to poor endothelial counts and the true extent of endothelial cell loss could be greater.

PDEK offers several advantages in terms of donor age, tissue handling and ease of the procedure especially related to unrolling of the tissue during transplantation. This study shows that the endothelial cell loss in PDEK tissue preparation is no worse than that observed in DMEK tissue preparation, ex vivo, by the bubbling technique. Though the Type-1 BB, which is the type required for PDEK, is obtained in over 80% of donor sclero-corneal discs it is difficult to predict which type of BB will be obtained in any given sclero-corneal disc. Thus, the surgeon

would need to be prepared to perform DMEK tissue if a Type-2 BB results during donor preparation for PDEK.

CHAPTER 7

CONCLUSION AND SUMMARY

Lamellar keratoplasty is the preferred option for several indications of corneal transplantation. Deep anterior lamellar keratoplasty (DALK) by the big bubble technique revealed clinical clues suggesting the existence of a defined layer in the deep stroma [8]. Simulation of DALK in donor eyes revealed different types of big bubbles and the presence of a compact, tough stromal layer that is impervious to air and has an absence/paucity of keratocytes. The layer was termed Pre-Descemets (Dua's) layer. Dua's layer has led to innovations in corneal surgery, namely triple-DALK pre-Descemets endothelial keratoplasty (PDEK), and suture management of acute hydrops [15] [8] [107].

In this thesis, Dua's layer characteristics were studied by air injection of sclera-corneal samples in simulating DALK. It was found that Dua's layer baring DALK can withstand high intraoperative pressures compared to Descemet's membrane baring DALK. Also, the dynamics of big bubble formation were studied in the context of the known architecture of the cornea stroma. It was found that the consistent pattern of passage of air is indicative of the architecture and microanatomy of the

corneal stroma where collagen lamellae are orthogonally arranged centrally and as a circular annulus at the periphery. The novel peripheral fenestrations explain the peripheral commencement of a type-2BB and the escape of air into the anterior chamber during DALK.

OCT characteristics of the different layers in the wall of the big bubbles were measured to help surgeons identify bubbles and understand the structures seen by intra-operative OCT.

The corneal endothelial cell density in PDEK tissue preparation was shown to be no worse, if not slightly better than, in DMEK tissue preparation by pneumodissection. PDEK preparation by pneumodissection has shown a viable graft preparation technique.

Zaki AA et al described a combination of DALK with phacoemulsification and lens implant, termed the DALK-Triple procedure. When confronted with patients requiring DALK who also had dense cataracts they were able to perform cataract surgery under the exposed DL of a type-1 BB. They reported that DL could withstand all pressure fluctuations associated with the phacoemulsification procedure and that despite stromal scarring requiring keratoplasty, the DL was remarkably clear in most cases [14]. In one instance they attempted DALK-Triple

under the DM (type-2 BB), which burst promptly during injection of viscoelastic in the anterior chamber.

In this study we reported the pressure and volume of air required to create the BB, the volume and pressure of air in type-1 BB and the bursting pressure of type-1 BB (Chapter 3). In the ex-vivo conditions of this study, it was possible to expand type-1BB to its bursting point by continued forceful injection of air with the needle positioned in the cavity of the bubble. This situation would simulate increased intraocular pressure exerted on the layers during phacoemulsification carried out under the layers (DALK-triple). The lowest pressure at which a type-1BB burst was 40 kpa and the highest was 110 kpa. The mean bursting pressure was 66.65 +/- 18.65 kpa. Although Dua et al reported the bursting pressure in the original paper [4], I refined the measurement by placing the needle tip in the type-1 BB while increasing the pressure to bursting point. This approach eliminated any variations induced by the resistance of the stroma to the passage of air. Any effect of variable leakage of air from the periphery of the sclero-cornea was prevented by the use of the clamp. In addition, the accuracy of the measurements was enhanced by using the continuous digital pressure recording device (Chapter 3).

When cataract and DALK surgery are required simultaneously; if the cornea is clear, one could consider performing phacoemulsificaton as the first step and DALK as the second step of the same procedure. However, when the cornea is scarred to an extent that visualisation is poor, a triple-DALK would be the preferred option. With triple-DALK, when air injection fails to produce a type-1BB, manual dissection allows access to the plane between the deep stroma and DL. Once the opaque cornea, related to the aeration of the stroma anterior the DL is removed, the transparent DL allows phacoemulsification to be carried out (Chapter 3).

At the corneal periphery, Dua's layer continues as the collagen core of the trabecular meshwork and is populated with trabecular cells. This may have implications for glaucoma that require further investigation [8]. With pneumodissection the type-1BB (cleavage between PDL and stroma) is common but often a type-2BB (cleavage between DM and PDL) or a mixed BB forms [4, 62]. Injected air traverses the thickness of the stroma and on reaching the posterior lamellae, lifts off the PDL, which is impervious to air [4, 62]. Very little is known of the path air traverses in the stroma before it reaches the respective planes to create a type-1, type-2 or mixed BB. We hypothesized that the path taken by injected air is determined by the corneal

stromal microarchitecture, which influences the type of BB formation (Chapter 4). In our study, I examined the movement of air injected in the stroma of human sclero-corneal discs to understand the dynamics of BB formation in the context of the corneal stromal architecture and microanatomy of the posterior cornea. I present evidence to explain the mechanisms of formation of the different types of BB (Chapter 4).

It was noted that some fenestrations are located distal to the attachment of the DM, between the termination of DM and the origin of the trabecular meshwork and at times between the trabecular meshwork and sclera. Air escaping from these holes would find access to the anterior chamber and is most likely the route through which air bubbles appear in the anterior chamber. Such holes or fenestrations between the termination of DM and trabecular meshwork were noted in all samples where peripheral leaking points were marked and studied by SEM.

This study shows that air moves in a consistent pattern in the corneal stroma, which corresponds to the known architecture and disposition of stromal collagen in the central and peripheral stroma. Spaces between interwoven lamellae appear to permit and direct intrastromal movement of air to the plane anterior to PDL and create a type-1BB. The demonstration of multiple clusters of fenestrations in the periphery of the PDL, adjacent to

the trabecular meshwork, is a novel addition to the microanatomy of the peripheral cornea and provides a valid explanation for the egress of air through PDL, to create a type-2 BB, and into the anterior chamber during DALK. Despite the initial controversy [16, 61] the lack of air-spaces in PDL and its impervious (to air) nature; the concentration of elastin fibres in PDL [74] and the fact that a type-1BB cannot be obtained following ablation of PDL by phototherapeutic keratectomy [79], and its recent demonstration in-vivo by ultrahigh resolution OCT [80], all point to its unique nature.

OCT characteristics of the posterior wall of the BB was also studied by using Fourier Domain-OCT (FD-OCT) and Time Domain-OCT (TD-OCT). It was found that FD-OCT of the posterior wall of type-1 (Dua's layer [DL] with DM) and type-2 BB (DM alone) both revealed a double-contour hyper-reflective curvilinear image with a hypo-reflective zone in between. The anterior line of type-2 BB was thinner than that seen with type-1 BB. In mixed BB, FD-OCT showed two separate curvilinear images. The anterior image was a single hyper-reflective line (DL) whereas the posterior image, representing the posterior wall of type-2 BB (DM) was made of two hyper-reflective lines with a dark space in between. TD-OCT images were similar with less defined component lines but the entire extent of the BB could be visualised.

Pre-Descemet's endothelial keratoplasty is another lamellar corneal transplant procedure wherein the donor graft is composed of pre-Descemet's membrane (Dua's layer) with Descemet's membrane and endothelium. This composite is transplanted after taking off the recipient's Descemet's membrane [43]. The fact that a Type-1 BB can be created in donors of any age (our unpublished observations) would allow very young tissue with consequent higher endothelial counts to be used for PDEK compared to the conventional stripping technique used to obtain tissue for DMEK wherein it is recognised that the risk of tissue loss is greater in older donors. [101, 102] Moreover the support afforded by DL makes the tissue easier to handle and unroll in the eye compared to DM alone. Agarwal et al [43] also demonstrated good graft attachment with good visual recovery post operatively. Four patients out of five, gained corrected distant visual acuity of 20/30 and one patient gained 20/40. These results suggested that endothelial cell function was adequate after PDEK [43] though they did not assess endothelial cell counts in their study.

In our study (Chapter 6) I aimed to provide objective evidence of endothelial cell counts by assessing endothelial cell loss that could result from the steps employed in preparation of PDEK

graft tissue and compare it with endothelial cell density of DMEK graft tissue obtained by the same technique (Chapter 6).

It was concluded, on the basis of this study, that the endothelial cell loss with PDEK tissue preparation is no worse than that with DMEK tissue preparation by the pneumo-dissection method. This coupled with the clinical results from PDEK observed so far would suggest that PDEK is a viable endothelial transplant procedure (Chapter 6).

BIBLIOGRAPHY

1. Marshall, J. and C.F. Grindle, *Fine structure of the cornea and its development.* Trans Ophthalmol Soc U K, 1978. **98**(3): p. 320-8.
2. Beuerman, R.W. and L. Pedroza, *Ultrastructure of the human cornea.* Microsc Res Tech, 1996. **33**(4): p. 320-35.
3. Jester, J.V., et al., *Lessons in corneal structure and mechanics to guide the corneal surgeon.* Ophthalmology, 2013. **120**(9): p. 1715-7.
4. Dua, H.S., et al., *Human corneal anatomy redefined: a novel pre-Descemet's layer (Dua's layer).* Ophthalmology, 2013. **120**(9): p. 1778-85.
5. Dua, H.S., et al., *The collagen matrix of the human trabecular meshwork is an extension of the novel pre-Descemet's layer (Dua's layer).* Br J Ophthalmol, 2014. **98**(5): p. 691-7.
6. Anthony J. Bron, Ramesh C. Tripathi, and B.J. Tripathi, *Wolff's Anatomy of thEye and Orbit*. Eighth edition ed. 1997: Chapman & Hall Medical.
7. Zinn, K.M. and S. Mockel-Pohl, *Fine structure of the developing cornea.* Int Ophthalmol Clin, 1975. **15**(1): p. 19-37.
8. Dua, H.S., L.A. Faraj, and D.G. Said, *Dua's layer: discovery, characteristics, clinical applications, controversy and potential relevance to glaucoma.* Expert Review of Ophthalmology, 2015. **10**(6): p. 531-547.
9. Thoft's, S.a., *The Cornea: Scientific Foundations and Clinical Practice*, ed. C.S. Foster., D.T. Azar, and C.H. Dohlman. 2005, USA: LippincottWilliams & Wilkins.
10. Al-Aqaba, M.A., et al., *Architecture and distribution of human corneal nerves.* Br J Ophthalmol, 2010. **94**(6): p. 784-9.
11. Navarro, R., J.J. Rozema, and M.J. Tassignon, *Orientation changes of the main corneal axes as a function of age.* Optom Vis Sci, 2013. **90**(1): p. 23-30.
12. A. R. Elkington, H. J. Frank, and M.J. Greaney, *Clinical Optics*. Third edition ed. 1999: Blackwell.
13. Lewis, P.N., et al., *Three-dimensional arrangement of elastic fibers in the human corneal stroma.* Exp Eye Res, 2015. **146**: p. 43-53.
14. Zaki, A.A., et al., *Deep anterior lamellar keratoplasty-triple procedure: a useful clinical application of the pre-Descemet's layer (Dua's layer).* Eye (Lond), 2014.
15. Yahia Cherif, H., et al., *Efficacy and safety of pre-Descemet's membrane sutures for the management of acute corneal hydrops in keratoconus.* Br J Ophthalmol, 2015. **99**(6): p. 773-7.
16. Schlotzer-Schrehardt, U., et al., *Ultrastructure of the posterior corneal stroma.* Ophthalmology, 2015. **122**(4): p. 693-9.
17. Patel, S.V., et al., *Automated quantification of keratocyte density by using confocal microscopy in vivo.* Invest Ophthalmol Vis Sci, 1999. **40**(2): p. 320-6.
18. Moffatt, S.L., V.A. Cartwright, and T.H. Stumpf, *Centennial review of corneal transplantation.* Clin Experiment Ophthalmol, 2005. **33**(6): p. 642-57.
19. Keenan, T.D., et al., *Trends in the indications for corneal graft surgery in the United Kingdom: 1999 through 2009.* Arch Ophthalmol, 2012. **130**(5): p. 621-8.
20. Reinhart, W.J., et al., *Deep anterior lamellar keratoplasty as an alternative to penetrating keratoplasty a report by the american academy of ophthalmology.* Ophthalmology, 2011. **118**(1): p. 209-18.
21. Sogutlu Sari, E., et al., *Penetrating keratoplasty versus deep anterior lamellar keratoplasty: comparison of optical and visual quality outcomes.* Br J Ophthalmol, 2012. **96**(8): p. 1063-7.
22. Tan, D.T., et al., *Corneal transplantation.* Lancet, 2012. **379**(9827): p. 1749-61.

23. Olson, R.J., et al., *Penetrating keratoplasty for keratoconus: a long-term review of results and complications.* J Cataract Refract Surg, 2000. **26**(7): p. 987-91.

24. Espandar, L. and A.N. Carlson, *Lamellar keratoplasty: a literature review.* J Ophthalmol, 2013. **2013**: p. 894319.

25. Anwar, M., *Dissection technique in lamellar keratoplasty.* Br J Ophthalmol, 1972. **56**(9): p. 711-3.

26. Sugita, J. and J. Kondo, *Deep lamellar keratoplasty with complete removal of pathological stroma for vision improvement.* Br J Ophthalmol, 1997. **81**(3): p. 184-8.

27. Melles, G.R., et al., *A technique to visualize corneal incision and lamellar dissection depth during surgery.* Cornea, 1999. **18**(1): p. 80-6.

28. Anwar, M. and K.D. Teichmann, *Big-bubble technique to bare Descemet's membrane in anterior lamellar keratoplasty.* J Cataract Refract Surg, 2002. **28**(3): p. 398-403.

29. Anwar, M. and K.D. Teichmann, *Deep lamellar keratoplasty: surgical techniques for anterior lamellar keratoplasty with and without baring of Descemet's membrane.* Cornea, 2002. **21**(4): p. 374-83.

30. Suwan-Apichon, O., et al., *Microkeratome versus femtosecond laser predissection of corneal grafts for anterior and posterior lamellar keratoplasty.* Cornea, 2006. **25**(8): p. 966-8.

31. McKee, H.D., et al., *Donor preparation using pneumatic dissection in endothelial keratoplasty: DMEK or DSEK?* Cornea, 2012. **31**(7): p. 798-800.

32. Price, M.O. and F.W. Price, Jr., *Descemet's membrane endothelial keratoplasty surgery: update on the evidence and hurdles to acceptance.* Curr Opin Ophthalmol, 2013. **24**(4): p. 329-35.

33. Sikder, S., et al., *Ultra-thin donor tissue preparation for endothelial keratoplasty with a double-pass microkeratome.* Am J Ophthalmol, 2011. **152**(2): p. 202-208 e2.

34. Phillips, P.M., et al., *"Ultrathin" DSAEK tissue prepared with a low-pulse energy, high-frequency femtosecond laser.* Cornea, 2013. **32**(1): p. 81-6.

35. van der Meulen, I.J., et al., *Correlation of straylight and visual acuity in long-term follow-up of manual descemet stripping endothelial keratoplasty.* Cornea, 2012. **31**(4): p. 380-6.

36. Arenas, E., et al., *Lamellar corneal transplantation.* Surv Ophthalmol, 2012. **57**(6): p. 510-29.

37. Tourtas, T., et al., *Descemet membrane endothelial keratoplasty versus descemet stripping automated endothelial keratoplasty.* Am J Ophthalmol, 2012. **153**(6): p. 1082-90 e2.

38. Rudolph, M., et al., *Corneal higher-order aberrations after Descemet's membrane endothelial keratoplasty.* Ophthalmology, 2012. **119**(3): p. 528-35.

39. Guerra, F.P., et al., *Endothelial keratoplasty: fellow eyes comparison of Descemet stripping automated endothelial keratoplasty and Descemet membrane endothelial keratoplasty.* Cornea, 2011. **30**(12): p. 1382-6.

40. Parker, J., et al., *Outcomes of Descemet membrane endothelial keratoplasty in phakic eyes.* J Cataract Refract Surg, 2012. **38**(5): p. 871-7.

41. Anshu, A., M.O. Price, and F.W. Price, Jr., *Risk of corneal transplant rejection significantly reduced with Descemet's membrane endothelial keratoplasty.* Ophthalmology, 2012. **119**(3): p. 536-40.

42. Naveiras, M., et al., *Causes of glaucoma after descemet membrane endothelial keratoplasty.* Am J Ophthalmol, 2012. **153**(5): p. 958-966 e1.

43.   Agarwal, A., et al., *Pre-Descemet's endothelial keratoplasty (PDEK).* Br J Ophthalmol, 2014.

44.   Panda, A., et al., *Corneal graft rejection.* Surv Ophthalmol, 2007. **52**(4): p. 375-96.

45.   Poon, A., et al., *Topical Cyclosporin A in the treatment of acute graft rejection: a randomized controlled trial.* Clin Experiment Ophthalmol, 2008. **36**(5): p. 415-21.

46.   Lim, S.H., *Clinical applications of anterior segment optical coherence tomography.* J Ophthalmol, 2015. **2015**: p. 605729.

47.   Ramos, J.L., Y. Li, and D. Huang, *Clinical and research applications of anterior segment optical coherence tomography - a review.* Clin Experiment Ophthalmol, 2009. **37**(1): p. 81-9.

48.   Izatt, J.A., et al., *Micrometer-scale resolution imaging of the anterior eye in vivo with optical coherence tomography.* Arch Ophthalmol, 1994. **112**(12): p. 1584-9.

49.   *Huang D, Li Y, Tang M. Interpretation of corneal images. in in Huang D,*

Duker S J, Fujimoto J G, Lumbroso B, Schuman, J. S. Weinreb R N , eds Imaging the Eye from Front to Back with RTVue Fourier-Domain optical Coherence Tomography. USA: SLACK Incorporated 2010: 39-46.

50.   Fujimoto JG, H.D., *Introduction to optical coherence tomography*. Imaging the Eye from Front to Back with RTVue Fourier-Domain optical Coherence Tomography. 2010, USA: SLACK Incorporated. 1-22.

51.   Drexler, W., et al., *Ultrahigh-resolution ophthalmic optical coherence tomography.* Nat Med, 2001. **7**(4): p. 502-7.

52.   Maurino, V., et al., *Fixed dilated pupil (Urrets-Zavalia syndrome) after air/gas injection after deep lamellar keratoplasty for keratoconus.* Am J Ophthalmol, 2002. **133**(2): p. 266-8.

53.   Dua, H.S., et al., *Biomechanica y arquitetura corneal (corneal architecture and biomechanics)*. null. Vol. null. 2014. 35.

54.   al, D.H.e., *dynamics of big bubble formation in deep anterior lamellar keratoplasty (DALK) by the big bubble technique. In vitro studies.* Acta Ophthalmol, 2017.

55.   Zhao, Y., et al., *Intraocular pressure and calculated diastolic ocular perfusion pressure during three simulated steps of phacoemulsification in vivo.* Invest Ophthalmol Vis Sci, 2009. **50**(6): p. 2927-31.

56.   Khng, C., et al., *Intraocular pressure during phacoemulsification.* J Cataract Refract Surg, 2006. **32**(2): p. 301-8.

57.   Vasavada, V., et al., *Real-time dynamic intraocular pressure fluctuations during microcoaxial phacoemulsification using different aspiration flow rates and their impact on early postoperative outcomes: a randomized clinical trial.* J Refract Surg, 2014. **30**(8): p. 534-40.

58.   Kamae, K.K., et al., *Intraocular pressure changes during injection of microincision and conventional intraocular lenses through incisions smaller than 3.0 mm.* J Cataract Refract Surg, 2009. **35**(8): p. 1430-6.

59.   Keane, M., et al., *Deep anterior lamellar keratoplasty versus penetrating keratoplasty for treating keratoconus.* Cochrane Database Syst Rev, 2014(7): p. CD009700.

60.   Jafarinasab, M.R., et al., *Dissection plane in deep anterior lamellar keratoplasty using the big-bubble technique.* Cornea, 2010. **29**(4): p. 388-91.

61.   McKee, H.D., et al., *Residual corneal stroma in big-bubble deep anterior lamellar keratoplasty: a histological study in eye-bank corneas.* Br J Ophthalmol, 2011. **95**(10): p. 1463-5.

62.   Ángeles del Buey Sayas MA and C.P.M. CP, *Biomechanica y arquitetura corneal (corneal architecture and biomechanics*. 2014: Elsevier.

63.   Goweida, M.B., *Intraoperative review of different bubble types formed during pneumodissection (big-bubble) deep anterior lamellar keratoplasty.* Cornea, 2015. **34**(6): p. 621-4.

64.   M, A., *Big Bubble technique*. Atlas of Lamellar Keratoplasty, ed. T.G. Fontana L, eds. 2007, San Giovan: Fabiano.

65.   Abahussin, M., et al., *3D collagen orientation study of the human cornea using X-ray diffraction and femtosecond laser technology.* Invest Ophthalmol Vis Sci, 2009. **50**(11): p. 5159-64.

66.   Meek, K.M. and C. Knupp, *Corneal structure and transparency.* Prog Retin Eye Res, 2015. **49**: p. 1-16.

67.   Butler, T.K., et al., *In vitro model of infectious crystalline keratopathy: tissue architecture determines pattern of microbial spread.* Invest Ophthalmol Vis Sci, 2001. **42**(6): p. 1243-6.

68.   Muller, L.J., E. Pels, and G.F. Vrensen, *The specific architecture of the anterior stroma accounts for maintenance of corneal curvature.* Br J Ophthalmol, 2001. **85**(4): p. 437-43.

69.   W, K., *Ubermechanisch-funktionelle strikuren des auges.* Albrech Vin Graefes Arch Ophthamol, 1938. **138**: p. 424-485.

70.   Newton, R.H. and K.M. Meek, *Circumcorneal annulus of collagen fibrils in the human limbus.* Invest Ophthalmol Vis Sci, 1998. **39**(7): p. 1125-34.

71.   Aghamohammadzadeh, H., R.H. Newton, and K.M. Meek, *X-ray scattering used to map the preferred collagen orientation in the human cornea and limbus.* Structure, 2004. **12**(2): p. 249-56.

72.   M'Ilroy J, H., *On the Presence of Elastic Fibres in the Cornea.* J Anat Physiol, 1906. **40**(Pt 3): p. 282-91.

73.   Asejczyk-Widlicka, M., et al., *Modelling the elastic properties of the anterior eye and their contribution to maintenance of image quality: the role of the limbus.* Eye (Lond), 2007. **21**(8): p. 1087-94.

74.   Lewis, P.N., et al., *Three-dimensional arrangement of elastic fibers in the human corneal stroma.* Exp Eye Res, 2016. **146**: p. 43-53.

75.   Liu, Z., et al., *Split of Descemet's membrane and pre-Descemet's layer in fungal keratitis: new definition of corneal anatomy incorporating new knowledge of fungal infection.* Histopathology, 2015. **66**(7): p. 1046-9.

76.   Smolek, M.K. and B.E. McCarey, *Interlamellar adhesive strength in human eyebank corneas.* Invest Ophthalmol Vis Sci, 1990. **31**(6): p. 1087-95.

77.   Dua, H.S. and D.G. Said, *Clinical evidence of the pre-Descemets layer (Dua's layer) in corneal pathology.* Eye (Lond), 2016. **30**(8): p. 1144-5.

78.   Dua, H.S., et al., *Author reply: To PMID 23714320.* Ophthalmology, 2014. **121**(5): p. e25-6.

79.   Dua, H.S., et al., *Big bubble deep anterior lamellar keratoplasty: the collagen layer in the wall of the big bubble is unique.* Acta Ophthalmol, 2015. **93**(5): p. 427-30.

80.   Bizheva, K., et al., *In Vivo Imaging and Morphometry of the Human Pre-Descemet's Layer and Endothelium With Ultrahigh-Resolution Optical Coherence Tomography.* Invest Ophthalmol Vis Sci, 2016. **57**(6): p. 2782-7.

81.   Dua, H.S., et al., *Differentiating type 1 from type 2 big bubbles in deep anterior lamellar keratoplasty.* Clin Ophthalmol, 2015. **9**: p. 1155-7.

82. Wylegala, E., et al., *Anterior segment imaging: Fourier-domain optical coherence tomography versus time-domain optical coherence tomography.* J Cataract Refract Surg, 2009. **35**(8): p. 1410-4.

83. Sharma, N., et al., *Anterior Segment Optical Coherence Tomography-Guided Management Algorithm for Descemet Membrane Detachment After Intraocular Surgery.* Cornea, 2015. **34**(9): p. 1170-4.

84. Guillermo Rocha, V.P., *Use of the Visante for Anterior Segment Ocu;ar Coherence Tomography.* Techniques in Ophthalmology, 2007. **5**(2): p. 67-77.

85. Dada, T., et al., *Comparison of anterior segment optical coherence tomography and ultrasound biomicroscopy for assessment of the anterior segment.* J Cataract Refract Surg, 2007. **33**(5): p. 837-40.

86. Wang, C., et al., *Comparison of Fourier-Domain and Time-Domain Optical Coherence Tomography in the Measurement of Thinnest Corneal Thickness in Keratoconus.* J Ophthalmol, 2015. **2015**: p. 402925.

87. Altaan, S.L., et al., *Endothelial cell loss following tissue harvesting by pneumodissection for endothelial keratoplasty: an ex vivo study.* Br J Ophthalmol, 2015. **99**(5): p. 710-3.

88. Shousha, M.A., et al., *Use of ultra-high-resolution optical coherence tomography to detect in vivo characteristics of Descemet's membrane in Fuchs' dystrophy.* Ophthalmology, 2010. **117**(6): p. 1220-7.

89. Christopoulos, V., et al., *In vivo corneal high-speed, ultra high-resolution optical coherence tomography.* Arch Ophthalmol, 2007. **125**(8): p. 1027-35.

90. Ferre, L.A., et al., *Optical coherence tomography anatomy of the corneal endothelial transplantation wound.* Cornea, 2010. **29**(7): p. 737-44.

91. Mencucci, R., et al., *Descemet stripping automated endothelial keratoplasty in Fuchs' corneal endothelial dystrophy: anterior segment optical coherence tomography and in vivo confocal microscopy analysis.* BMC Ophthalmol, 2015. **15**: p. 99.

92. Siebelmann, S., et al., *Intraoperative Optical Coherence Tomography in Children with Anterior Segment Anomalies.* Ophthalmology, 2015.

93. Ide, T., et al., *Intraoperative use of three-dimensional spectral-domain optical coherence tomography.* Ophthalmic Surg Lasers Imaging, 2010. **41**(2): p. 250-4.

94. M., A., *Big-Bubble technique*, in *Atlas of Lamellar Keratoplasty*, T.G. Fontana L, eds., Editor. 2007, Fabiano: San Giovani, Italy. p. 125-36.

95. Busin, M., et al., *Stromal support for Descemet's membrane endothelial keratoplasty.* Ophthalmology, 2010. **117**(12): p. 2273-7.

96. Busin, M., et al., *Pneumatic dissection and storage of donor endothelial tissue for Descemet's membrane endothelial keratoplasty: a novel technique.* Ophthalmology, 2010. **117**(8): p. 1517-20.

97. Busin, M., et al., *Donor tissue preparation for Descemet membrane endothelial keratoplasty.* Br J Ophthalmol, 2011. **95**(8): p. 1172-3; author reply 1173.

98. Zarei-Ghanavati, S., H. Khakshoor, and M. Zarei-Ghanavati, *Reverse big bubble: a new technique for preparing donor tissue of Descemet membrane endothelial keratoplasty.* Br J Ophthalmol, 2010. **94**(8): p. 1110-1.

99. Dua, H.S. and D.G. Said, *Much froth over bubbles.* Br J Ophthalmol, 2011. **95**(8): p. 1041-2.

100. Studeny, P., et al., *Descemet membrane endothelial keratoplasty with a stromal rim (DMEK-S).* Br J Ophthalmol, 2010. **94**(7): p. 909-14.

101. Gorovoy, I.R., Q.N. Cui, and M.S. Gorovoy, *Donor tissue characteristics in preparation of DMEK grafts.* Cornea, 2014. **33**(7): p. 683-5.

102. Heinzelmann, S., et al., *Influence of donor characteristics on descemet membrane endothelial keratoplasty.* Cornea, 2014. **33**(6): p. 644-8.

103. Borderie, V.M., et al., *Long-term results of deep anterior lamellar versus penetrating keratoplasty.* Ophthalmology, 2012. **119**(2): p. 249-55.

104. Cheng, Y.Y., et al., *Endothelial cell loss and visual outcome of deep anterior lamellar keratoplasty versus penetrating keratoplasty: a randomized multicenter clinical trial.* Ophthalmology, 2011. **118**(2): p. 302-9.

105. Yoeruek, E., et al., *Comparison of pneumatic dissection and forceps dissection in Descemet membrane endothelial keratoplasty: histological and ultrastructural findings.* Cornea, 2012. **31**(8): p. 920-5.

106. Parekh, M., et al., *Descemet membrane endothelial keratoplasty tissue preparation from donor corneas using a standardized submerged hydro-separation method.* Am J Ophthalmol, 2014. **158**(2): p. 277-285 e1.

107. Zaki, A.A., et al., *Deep anterior lamellar keratoplasty--triple procedure: a useful clinical application of the pre-Descemet's layer (Dua's layer).* Eye (Lond), 2015. **29**(3): p. 323-6.